[CANCER RESEARCH 64, 3545–3549, May 15, 2004]

Expression of a Novel Human Gene, *Human Wings Apart-Like (hWAPL)*, Is Associated with Cervical Carcinogenesis and Tumor Progression

Kosuke Oikawa,[1,3,4] Tetsuya Ohbayashi,[1,3,4] Tohru Kiyono,[5] Hirotaka Nishi,[2] Keiichi Isaka,[2] Akihiro Umezawa,[4,6] Masahiko Kuroda,[1,3,4] and Kiyoshi Mukai[1]

Departments of [1]Pathology and [2]Obstetrics-Gynecology, Tokyo Medical University, Shinjuku-ku, Tokyo; [3]Core Research for Evolutional Science and Technology Research Project, Japan Science and Technology Corp., Kawaguchi-shi, Saitama; [4]Shinanomachi Research Park, Keio University, Shinjuku-ku, Tokyo; [5]Division of Virology, National Cancer Center Research Institute, Chuo-ku, Tokyo; and [6]National Research Institute for Child Health and Development, Setagaya-ku, Tokyo, Japan

ABSTRACT

In *Drosophila melanogaster*, the *wings apart-like* (*wapl*) gene encodes a protein that regulates heterochromatin structure. Here, we characterize a novel human homologue of *wapl* (termed *human WAPL*; *hWAPL*). The *hWAPL* mRNA was predominantly expressed in uterine cervical cancer, with weak expression in all other normal and tumor tissues examined. hWAPL expression in benign epithelia was confined to the basal cell layers, whereas in dysplasias it increasingly appeared in more superficial cell layers and showed a significant correlation with severity of dysplasia. Diffuse hWAPL expression was found in all invasive squamous cell carcinomas examined. In addition, NIH3T3 cells overexpressing hWAPL developed into tumors on injection into nude mice. Furthermore, repression of *hWAPL* expression by RNA interference induced cell death in SiHa cells. These results demonstrate that hWAPL is associated with cell growth, and the *hWAPL* expression may play a significant role in cervical carcinogenesis and tumor progression.

INTRODUCTION

The *wings apart-like* (*wapl*) gene of *Drosophila melanogaster* encodes a protein that regulates heterochromatin structure (1). Mutations of *wapl* prevent the normal close apposition of sister chromatids in heterochromatin regions but do not appear to affect either heterochromatin condensation or chromosomal segregation (1). This evidence suggests that *wapl* is required to hold sister chromatids together in mitotic heterochromatin. *wapl* has also been implicated in both heterochromatin pairing during female meiosis and the modulation of position effect variegation (1). In addition, a *P* element screen of *Drosophila* identified *wapl* as a modifier of chromosome inheritance (2).

Among all varieties of cancer, uterine cervical cancer is unique because of its association with high-risk human papillomavirus (HPV) infection, with strains like HPV-16 and HPV-18. High-risk HPVs encode two oncoproteins, E6 and E7, which subvert crucial cellular regulatory mechanisms that reactivate and maintain DNA synthesis in the host cell. E6 accelerates proteosomal degradation of the p53 tumor suppressor, and E7 inactivates the retinoblastoma protein, interfering with the action of both $p16^{INK4a}$ (3) and the cyclin-dependent kinase inhibitor $p21^{Cip1}$ (4, 5). Both the E6 and E7 high-risk HPV oncoproteins independently induce genomic instability in normal human cells (6, 7). Only a small portion of precursor lesions infected with HPV, however, develops into invasive carcinomas (8). Therefore, additional genetic and microenvironmental factors subsequent to HPV infection are thought to play an important role in the initiation and progression of cervical neoplasia (8–10).

In this study, we describe the isolation and characterization of a novel human *wapl*-related gene termed *human WAPL* (*hWAPL*). We have also demonstrated that *hWAPL* has the characteristics of an oncogene and is associated with uterine cervical cancer.

MATERIALS AND METHODS

cDNA Cloning and Construction of the hWAPL Expression Vector. To isolate the complete *hWAPL* cDNA sequence, we used a human testis Marathon-Ready cDNA kit (Clontech, Palo Alto, CA).

To create an expression vector encoding *hWAPL*, a *Hin*dIII-*Eco*RI cDNA fragment containing the complete coding region of hWAPL was amplified by PCR using the primers 5′-TTAAGCTTTGAAACTGGTGTCAAAATGACATCCAGATT-3′ and 5′-TTGAATTCAAGCAATGTTCCAAATATTCAATCACTCTAGAG-3′ and inserted into the hemagglutinin (HA)-tagged mammalian expression vector, pHM6 (HA-hWAPL; Roche Diagnostics, Mannheim, Germany).

Northern Blot and Quantitative Real-Time PCR Analysis. RNA isolation (11) and Northern blot analysis (11, 12) were performed as described. The 674-bp *Dpn*II fragment of *hWAPL* cDNA was used as a probe and labeled with ^{32}P using the Rediprime II random prime labeling system (Amersham Biosciences, Piscataway, NJ). A human β-actin cDNA control probe (Clontech) was used as a control.

First-strand cDNA synthesis was performed as described (13). Real-time PCR analysis was performed using the Smart Cycler System (Cepheid, Sunnyvale, CA) with SYBR Green I (Cambrex, Washington, DC). Real-time PCR used the *hWAPL*-specific primers 5′-GAATTCATAGGCACAGCGCTGAACTGTGTG-3′ and 5′-TTGAATTCCTAGCAATGTTCCAAATATTCA-3′ and β-actin-specific primers 5′-GGGAAATCGTGCGTGACATTAAG-3′ and 5′-TGTGTTGGCGTACAGGTCTTTG-3′. Reaction mixtures were denatured at 95°C for 30 s and then were subjected to 40 PCR cycles at 95°C for 3 s, 68°C for 30 s, and 87°C for 6 s. *hWAPL* mRNA levels were normalized to β-actin signals.

Immunohistochemistry and Immunoblot Analysis. To generate mouse monoclonal antibodies against hWAPL, we immunized mice against a 6 × histidine-tagged hWAPL COOH terminus (amino acids 814-1037) fusion protein. Spleen cells of an immunized mouse were fused with P3UI mouse myeloma cells as described previously (14). Of the 128 hybrids generated, one clone (clone R929) showed exclusive reactivity with hWAPL by ELISA. We used the supernatant of this clone as anti-hWAPL antibody.

Immunohistochemical assays were performed on formalin-fixed, paraffin-embedded sections using Ventana HX System Benchmark (Ventana Medical Systems Inc., Tucson, AZ). Immunohistochemical stains for hWAPL were interpreted semiquantitatively by assessing the intensity and extent of staining on the entire tissue sections present on the slides as described (9).

Immunoblot analyses were performed as described previously (15). The anti-HA (Roche Diagnostics; 3F10) and monoclonal anti-α-tubulin clone B-5-1-2 (Sigma Chemical Co., St. Louis, MO; T-5168) antibodies were purchased.

Animals and Treatment. BALB/cAJc1-nu female mice (4 weeks old) were purchased from Charles River Japan, Inc. (Kanagawa, Japan).

The tumorigeneicity of the stable NIH3T3 transformants overexpressing hWAPL *in vivo* was examined as described previously (16).

Cell Culture and small interfering RNA (siRNA) Transfection. SiHa and NIH3T3 cells were grown in DMEM (Sigma) containing 10% fetal bovine serum at 37°C in a 5% CO_2 environment. For the transfection of siRNA, we

Received 12/8/03; revised 3/15/04; accepted 3/16/04.

Grant support: Grant-in-Aid for Scientific Research on Priority Area (C) and Grant-in-Aid for Encouragement of Young Scientists from the Ministry of Education, Culture, Sports, Science and Technology, Japan, and a grant from Core Research for Evolutional Science and Technology, Japan Science and Technology Corp.

The costs of publication of this article were defrayed in part by the payment of page charges. This article must therefore be hereby marked *advertisement* in accordance with 18 U.S.C. Section 1734 solely to indicate this fact.

Note: T. Ohbayashi is currently at the Horizontal Medical Research Organization, Kyoto University Faculty of Medicine, Kyoto, Japan.

Requests for reprints: Masahiko Kuroda, Department of Pathology, Tokyo Medical University, 6-1-1, Shinjuku, Shinjuku-ku, Tokyo, 160-8402, Japan. Fax: 81-3-3352-6335; E-mail: kuroda@tokyo-med.ac.jp.

generated siRNAs using a Silencer siRNA Construction Kit (Ambion, Austin, TX). siRNA transfection was performed in DMEM without serum using Oligofectamine Reagent (Invitrogen Japan, Tokyo, Japan) and Opti-MEM I (Invitrogen Japan).

For cell quantitation, we harvested the cells from the wells of a 12-well plate and resuspended them in 100 μl of PBS. Trypan blue solution (100 μl, 0.4%; Sigma) was added to each sample, and viable cell numbers were quantitated using an erythrometer. The results shown are representative of three independent cell count analyses.

RESULTS

Molecular Cloning of *hWAPL*. To isolate *wapl*-related genes from human cells, we searched DNA databases and identified a cDNA fragment, KIAA0261 (17), and three expressed sequence tag clones, BE410177, BF79516, and BE257022, containing the KIAA0261 sequence. We also performed 5′ rapid amplification of cDNA ends. From these DNA sequences, we cloned and confirmed the full-length coding region sequence of the cDNA containing KIAA0261. We named this gene *hWAPL* (GenBank accession no. AB065003) to reflect its homology to *wapl*. The *hWAPL* gene product shows high sequence similarity in the WAPL-conserved region (amino acids 627-1169, 34% identical and 56% similar) and low similarity throughout the other regions to the *wapl* gene product. Several additional stretches of amino acids are also present in wapl protein (Fig. 1*A*).

High-Level Expression of hWAPL in Human Cervical Cancer. As *wapl* is involved in sister chromatid cohesion, hWAPL may modify chromosomal inheritance. Deregulation of the expression of genes involved in chromosomal inheritance directly induces a variety of disorders associated with aneuploidy, including birth defects and cancer. Northern blot analysis detected *hWAPL* mRNA expression in several invasive cervical cancer samples, examined in tandem with additional human cancers and normal tissues (Fig. 1*B*). We confirmed the *hWAPL* expression in cervical cancers by quantitative real-time PCR analysis of tumor and normal tissue samples. The levels of *hWAPL* mRNA expression in cervical cancers were significantly higher than the levels observed in either normal cervical controls or endometrial, ovarian, breast, lung, stomach, renal, and colon cancers (Fig. 1*C*).

To investigate the connection between hWAPL expression and oncogenesis in cervical malignancies, we examined the expression of hWAPL by immunohistochemistry in a series of clinical samples of the various grades of cervical dysplasia [cervical intraepithelial neoplasia (CIN) I–III] and invasive squamous cell carcinoma. We found nuclear immunostaining for hWAPL in all samples (Fig. 2*A*). hWAPL expression in benign squamous epithelia was confined to the basal and parabasal cell layers. In contrast, hWAPL expression in squamous dysplasia and invasive carcinoma increasingly appeared in the more superficial cell layers and was significantly increased compared with the adjacent benign epithelia ($P = 0.0002$ for CIN I, $P = 0.0003$ for CIN II, $P = 0.0001$ for CIN III, and $P = 0.0001$ for invasive squamous cell carcinoma; Wilcoxon's signed rank test). CIN I and II cases showed hWAPL expression in the basal 50 and 70% of the epithelial thickness, respectively, whereas CIN III and invasive squamous cell carcinoma showed hWAPL expression in the full thickness of the dysplastic epithelia (Fig. 2*A*). Furthermore, the mean hWAPL staining score increased remarkably with increasing grade of dysplasia (Fig. 2*B*). These data strongly suggest that the unscheduled high-level expression of hWAPL may play a significant role in cervical carcinogenesis and tumor progression.

hWAPL Has Oncogenic Characteristics. Because we observed high-level expression of *hWAPL* in tumors, we sought to determine whether hWAPL overexpression promotes tumor development. We transfected NIH3T3 cells with an HA-tagged hWAPL expression vector (HA-hWAPL 3T3) or HA expression vector (HA-3T3). Then, we compared the ability of HA-hWAPL 3T3 with HA-3T3 cells to grow as tumors in nude mice. We injected 10^6 cells into three s.c. sites of each nude mouse. HA-hWAPL 3T3 cells produced tumors in all nude mice within 10 days after injection of cells (100%, $n = 18$; Fig. 3*A*). HA-3T3 failed to produce tumors in any mice (0%, $n = 18$). We confirmed high hWAPL expression levels in the resultant tumors by Western blot analysis (Fig. 3*B*). These results suggest that *hWAPL* has the characteristics of an oncogene.

Repression of hWAPL Expression Induces Cell Death. We examined hWAPL function by suppressing hWAPL expression. Initial attempts to generate a *WAPL*-deficient mouse demonstrated that the loss of *WAPL* was embryonic lethal (data not shown). Therefore, we designed two 21-nucleotide, double-stranded siRNAs, siRNA(I) and siRNA(II), to repress *hWAPL* expression (Refs. 18 and 19; Figs. 1*A*

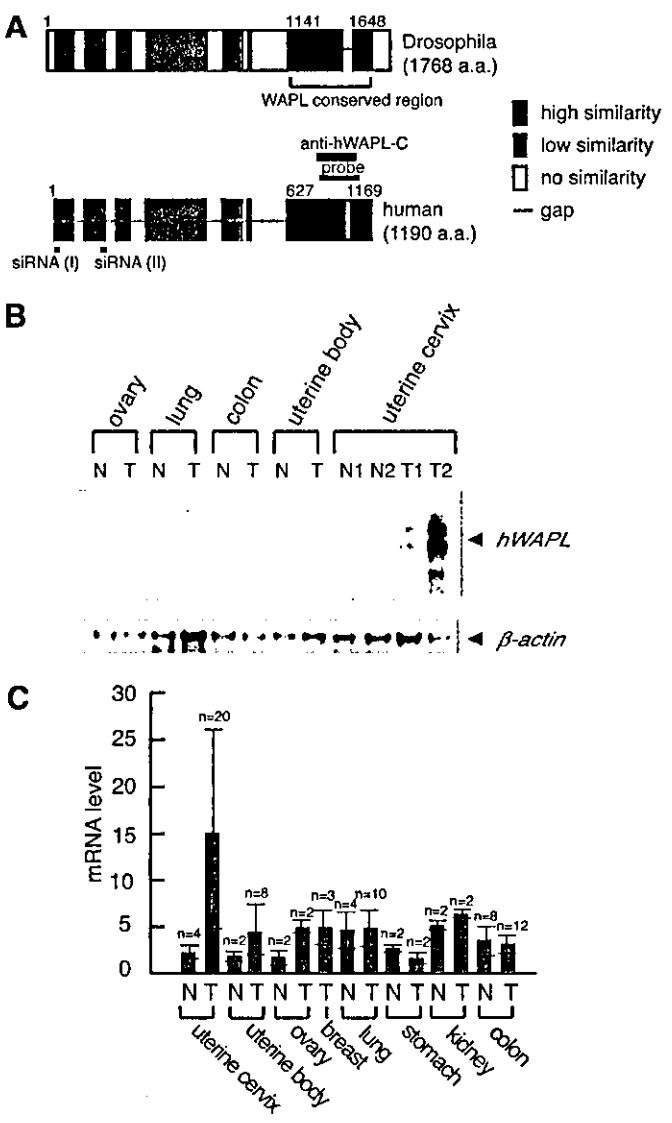

Fig. 1. Structures of wings apart-like (*WAPL*) proteins and *human WAPL* (*hWAPL*) expression in normal and tumor human tissues. *A*, schematic structure of the *hWAPL* and *Drosophila wapl* gene products. The site corresponding to the probe sequence used for Northern blot analysis is indicated by "probe." The antibody recognition site is indicated by "hWAPL-C." The small interfering RNA (*siRNA*) targeting sites are indicated by "siRNA(I)" and "siRNA(II)." *B*, Northern blot analysis of *hWAPL* in several normal (*N*) and tumor (*T*) human tissues. *C*, quantitative real-time PCR analysis demonstrating *hWAPL* mRNA levels in various normal (*N*) and tumor (*T*) human tissues. *Columns*, the means of examined samples. The minimum mRNA expression level was arbitrarily set to 1 in the graphical presentation; all other mRNA signals were normalized to this value. *Bars*, SD.

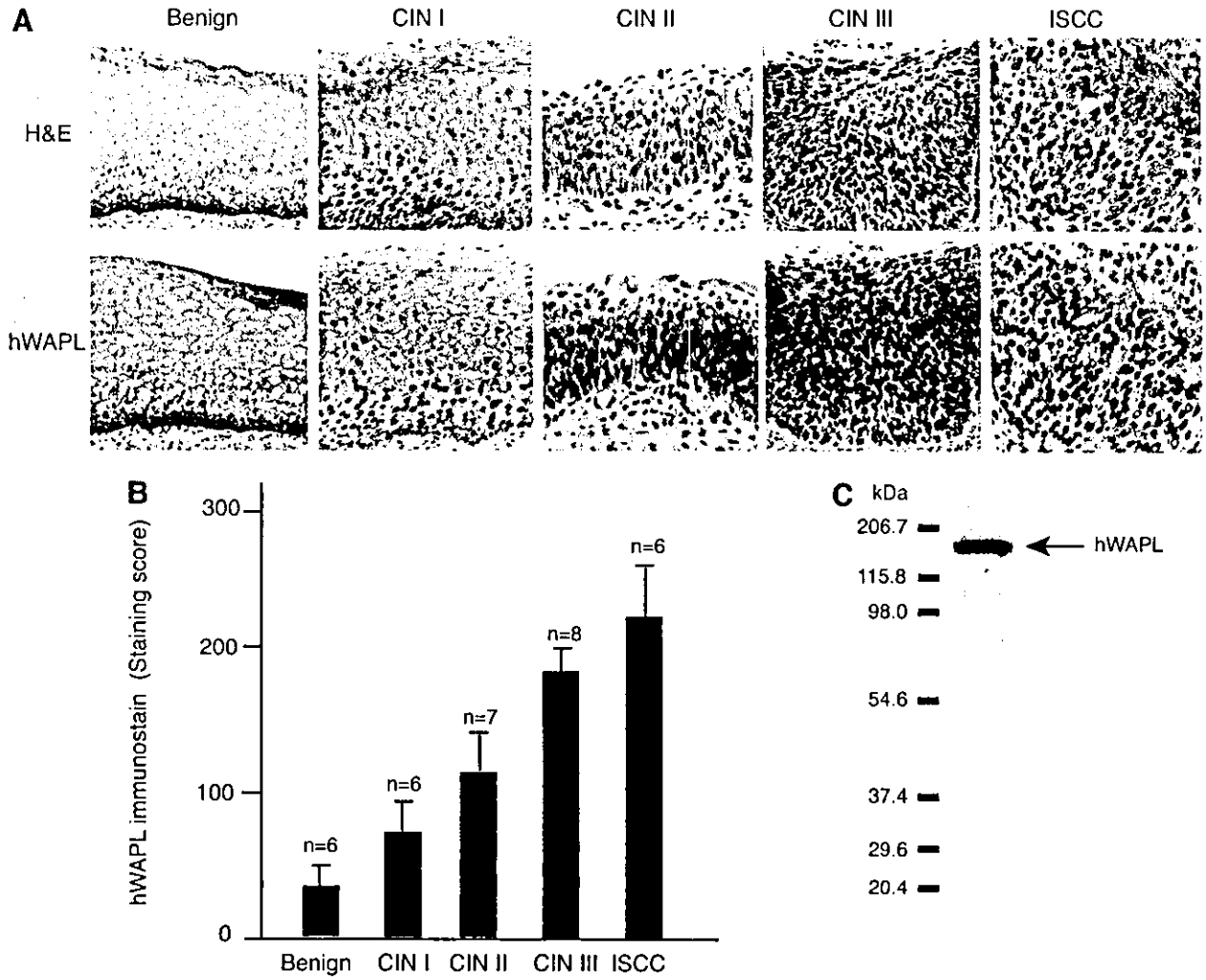

Fig. 2. Immunohistochemical analysis of human wings apart-like (*hWAPL*) expression in uterine cervical epithelia of normal, dysplasia, and carcinoma. *A*, immunohistochemical staining of hWAPL expression in benign squamous epithelium, various grades of squamous dysplasia [cervical intraepithelial neoplasia (*CIN*) grades I, II, and III], and invasive squamous cell carcinoma (*ISCC*). hWAPL was stained with hematoxylin counterstain; H&E, *B*, graphical representation of the increase of the hWAPL expression with increasing severity of dysplasia in cervical squamous epithelia. The mean hWAPL staining scores were calculated as described (9). *Bars*, SD. *C*, Western blot analysis with the total extract from a uterine cervical cancer-derived cell line, SiHa, to confirm the specificity of the anti-hWAPL monoclonal antibody hWAPL-C.

and 4*A*). We examined various human cancer-derived cell lines and found that cervical cancer-derived cell lines containing both HPV-positive and -negative cells exhibited higher levels of hWAPL expression compared with the other cell lines (data not shown). Then, we examined the effects of suppressing *hWAPL* in a cervical cancer-derived cell line, SiHa. siRNA transfection at a concentration of either 1 nM siRNA(I) or siRNA(II) reduced *hWAPL* mRNA levels (Fig. 4*B*). siRNA(I) was more effective at reducing *hWAPL* mRNA than siRNA(II). Thus, we used siRNA(I) in the subsequent experiments. hWAPL protein levels were also significantly reduced after siRNA(I) transfection (Fig. 4*C*). Interestingly, siRNA(I) repressed the growth of the cells and subsequently induced cell death (Fig. 4, *D* and *E*). siRNA(II) repressed cell growth in a similar manner as siRNA(I) (Fig. 4*D*), suggesting that the effects of these siRNAs on proliferation and viability are likely caused by the repression of *hWAPL* expression. Similar results were obtained in another cervical cancer-derived cell line, CaSki, with 10 nM siRNA(I) (data not shown). On the contrary, we did not observe any effects of siRNA(I) on cells expressing relatively low levels of *hWAPL*, such as Saos-2 and HCT116 (data not shown).

To investigate the fate of cells transfected with siRNA(I), we analyzed siRNA-transfected cells by flow cytometry (Fig. 5). In siRNA(I)-transfected cells, the population of cells exhibiting S phase DNA content increased (Fig. 5; 48 and 72 h). In addition, there was an increase in the number of apoptotic cells exhibiting subG$_1$ DNA content (Fig. 5; 72 h). Many cells showing S phase DNA content may also be apoptotic cells at G$_2$-M phase. Taken together, these results suggest that a malfunction in the hWAPL pathway activates an S phase checkpoint or another apoptotic pathway and consequently leads to cell death.

DISCUSSION

In this study, we report the isolation and characterization of a novel human gene termed *hWAPL*. We were unable to identify additional genes similar to *wapl* within the human genome sequence database. Thus, although the high-sequence conservation between hWAPL and wapl is limited to a third of the protein sequence encoded by *wapl* (Fig. 1*A*), we consider hWAPL to be the human homologue of wapl. We did not find any protein sequence motifs in hWAPL, except for the WAPL-conserved region (Fig. 1*A*). We therefore expect that hWAPL has similar functions to the wapl protein. Two hybridization signals for *hWAPL* were visible by Northern blot analysis (Fig. 1*B*). Western blot analysis, however, detected only a single band for

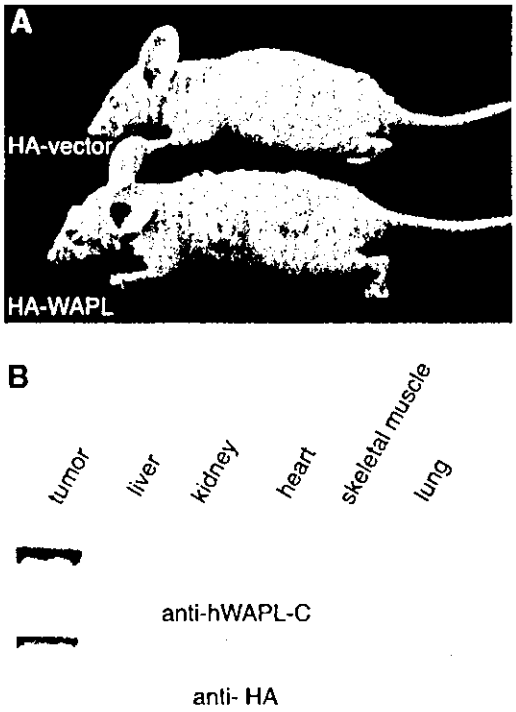

Fig. 3. Human wings apart-like (*hWAPL*) overexpression promotes tumor development. *A*, tumorigenecity of HA-hWAPL-3T3 in nude mice. The lower mouse in the *panel* is shown 10 days after the injection of HA-hWAPL-3T3 at three s.c. sites. The upper mouse was injected with the control HA-3T3 cells. *B*, Western blot analysis of hWAPL protein in tumor and other control tissues from HA-hWAPL-3T3-injected nude mice. *Top panel*, anti-hWAPL antibody; *bottom panel*, anti-HA antibody.

hWAPL (Fig. 2*C*). In addition, we did not obtain additional nucleotide sequences similar to the open reading frame of *hWAPL* by PCR analysis with various PCR primers (data not shown). Thus, we consider that the two hybridization signals may reflect the difference of the length of the untranslated regions of the *hWAPL* mRNA.

High-level expression of *hWAPL* was observed in cervical cancers (Fig. 1, *B* and *C*). Furthermore, hWAPL-overexpressing 3T3 cells developed into tumors on injection into nude mice (Fig. 3). These results suggest that *hWAPL* has oncogenic characteristics. Cervical cancer is a serious health problem, with ~500,000 women developing the disease each year worldwide. In many developing countries, it is the most common cause of cancer death and years of life lost because of cancer (20). Although the fundamental role of high-risk HPV infection in the pathogenesis of cervical carcinoma is well established, other factors are thought to play a role in cervical carcinogenesis (8, 21). Because all of uterine cervical samples examined were HPV positive (data not shown), it is still to be confirmed whether hWAPL expression is inducible by HPV infection. However, HPV-positive normal cervical tissue samples exhibited low hWAPL expression (Fig. 1, *B* and *C* and data not shown), and an HPV-negative, uterine cervical cancer-derived cell line, C33A, showed high hWAPL expression (data not shown). Thus, hWAPL expression is likely to be more closely related with cervical carcinogenesis than HPV infection. Recently, Aes *et al.* (9) found significant correlation among expression of Epo receptor, $p16^{INK4a}$, and *bcl*-2 in benign and dysplastic squamous epithelia. In our results, hWAPL showed similar expression pattern to Epo receptor and $p16^{INK4a}$ in benign and dysplastic cervical squamous epithelia and invasive squamous cell carcinomas (Fig. 2, *A* and *B*). Although we did not find any evidence for hWAPL being involved in hypoxia-inducible Epo signaling, hWAPL may cooperate with the Epo signaling in the progression of cervical neoplasia. These observations indicate that hWAPL overexpression can be used as a useful diagnostic tool in the detection of cervical dysplasia like $p16^{INK4a}$ (22) and Epo receptor (9). In addition, our results provide the necessity to investigate the potential of hWAPL as a cancer therapeutic target.

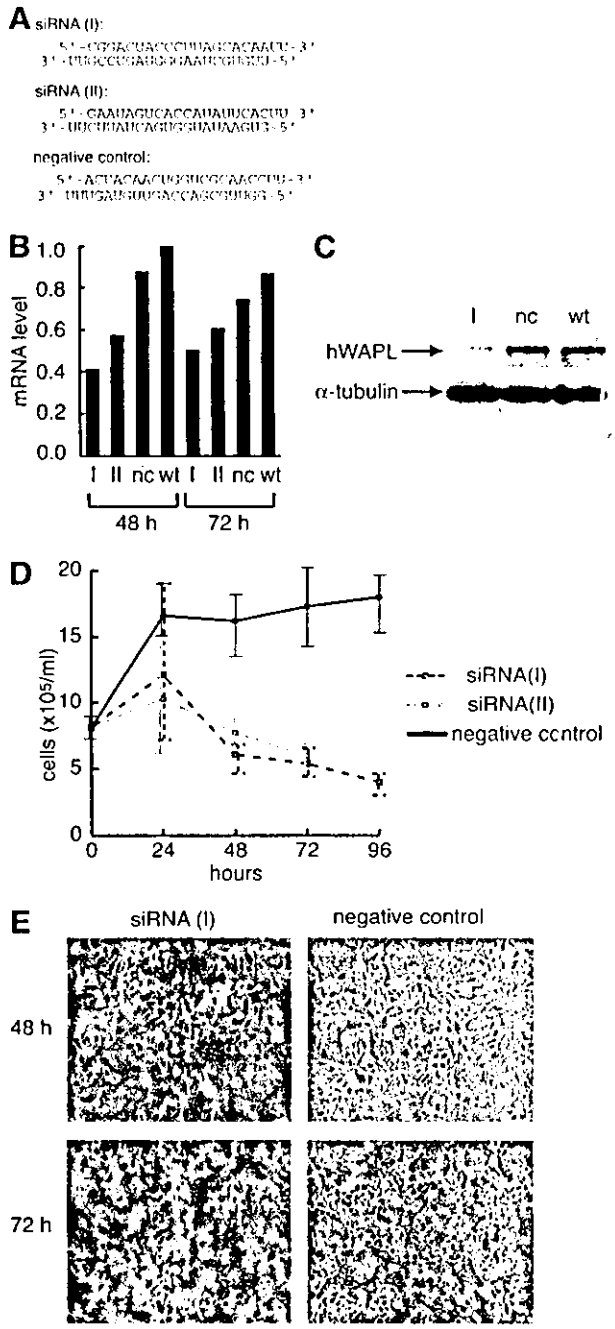

Fig. 4. Repression of human wings apart-like (*hWAPL*) expression by small interfering RNA (*siRNA*) treatment induces cell death. *A*, sequences and structures of siRNAs. The negative control siRNA possesses the same nucleotide composition as siRNA(I) but lacks homology to any known human genes. *B*, reduction of the *hWAPL* transcript by siRNA in SiHa cells. After siRNA transfection, SiHa cells were harvested at either 48 or 72 h. Total RNA was extracted from the cells and subjected to real-time PCR analysis. *I*, siRNA(I); *II*, siRNA(II); *nc*, negative control siRNA; *wt*, untransfected wild type. Data were normalized to a maximum mRNA level that was arbitrarily set to 1 in the graphical presentation. *C*, reduction of hWAPL protein levels by siRNA. Western blot analysis of total cell extracts from untreated SiHa or SiHa cells 72 h after transfection with siRNA(I) or negative control siRNA. α-tubulin is shown as a loading control. *D*, active siRNA specific for *hWAPL* induces cell death. SiHa cells transfected with siRNA(I), siRNA(II), or negative control siRNA were harvested at 24, 48, 72, and 96 h after transfection. Cell numbers were counted using an erythrometer. *Bars*, SE. *E*, representative phase-contrast images of SiHa cells transfected with siRNA(I) and negative control siRNA are shown.

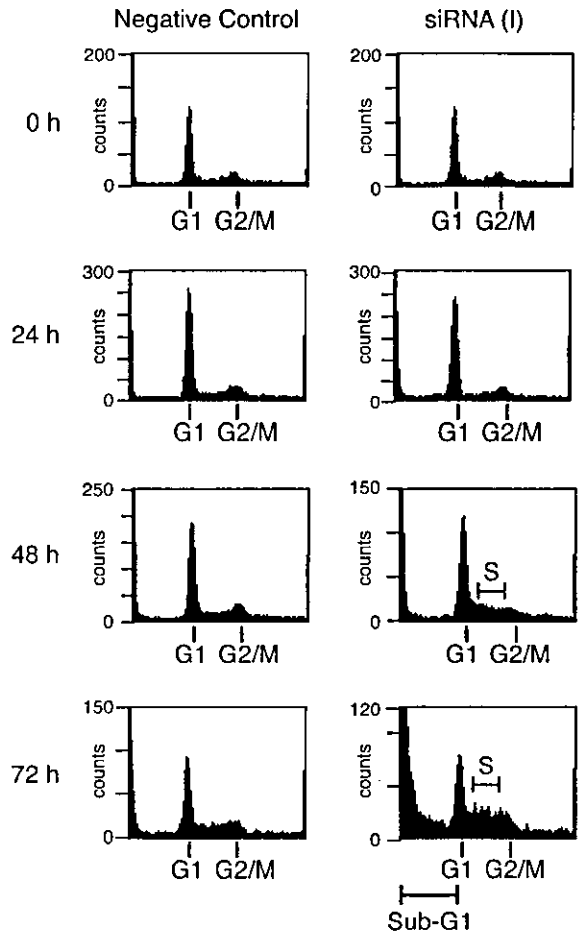

Fig. 5. Flow cytometric analysis of SiHa cells after small interfering RNA (*siRNA*) transfection. SiHa cells were transfected with either siRNA(I) or negative control siRNA, then harvested at 24, 48, and 72 h after transfection. Cells were stained with propidium iodide and subjected to flow cytometric analysis to examine DNA content. A total of 50,000 cells was counted for the sample siRNA(I) 72 h, and 20,000 cells were counted for the other samples.

Loss of WAPL was embryonic lethal in mouse (data not shown), and repression of hWAPL expression in SiHa cells led to cell death (Fig. 4). Flow cytometry analysis demonstrated that malfunction of hWAPL may cause apoptosis and/or arrest of cells at S phase (Fig. 5). In addition, *Drosophila wapl* is associated with regulation of chromatin organization (1). Thus, we expect that hWAPL is also associated with regulation of chromatin structure, and deregulation of hWAPL expression may induce chromosomal instability. Although additional investigations are necessary to elucidate the actual function of hWAPL in normal and malignant cells, our results have demonstrated that the novel oncogene, *hWAPL*, is one of the essential genes for development and cell growth and may play a significant role for cervical carcionogenesis and tumor progression.

ACKNOWLEDGMENTS

We thank K. Yoshida, R. Iwata, R. Tsujimoto, K. Kitamura, M. Sugiura, and M. Takaoka for their technical assistance.

REFERENCES

1. Verni F, Gandhi R, Goldberg ML, Gatti M. Genetic and molecular analysis of wings apart-like (wapl), a gene controlling heterochromatin organization in Drosophila melanogaster. Genetics 2000;154:1693–710.
2. Dobie KW, Kennedy CD, Velasco VM, et al. Identification of chromosome inheritance modifiers in Drosophila melanogaster. Genetics 2001;157:1623–37.
3. Kiyono T, Foster SA, Koop JI, McDougall JK, Galloway DA, Klingelhutz AJ. Both Rb/p16^{INK4a} inactivation and telomerase activity are required to immortalize human epithelial cells. Nature 1998;396:84–8.
4. Jones DL, Alani RM, Munger K. The human papillomavirus E7 oncoprotein can uncouple cellular differentiation and proliferation in human keratinocytes by abrogating p21^{Cip1}-mediated inhibition of cdk2. Genes Dev 1997;11:2101–11.
5. zur Hausen H. Papillomavirus infections–a major cause of human cancers. Biochim Biophys Acta 1996;1288:F55–78.
6. Hashida T, Yasumoto S. Induction of chromosome abnormalities in mouse and human epidermal keratinocytes by the human papillomavirus type 16 E7 oncogene. J Gen Virol 1991;72:1569–77.
7. White AE, Livanos EM, Tlsty TD. Differential disruption of genomic integrity and cell cycle regulation in normal human fibroblasts by the HPV oncoproteins. Genes Dev 1994;8:666–77.
8. Milde-Langosch K, Riethdorf S, Loning T. Association of human papillomavirus infection with carcinoma of the cervix uteri and its precursor lesions: theoretical and practical implications. Virchows Arch 2000;437:227–33.
9. Acs G, Zhang PJ, McGrath CM, et al. Hypoxia-inducible erythropoietin signaling in squamous dysplasia and squamous cell carcinoma of the uterine cervix and its potential role in cervical carcinogenesis and tumor progression. Am J Pathol 2003; 162:1789–806.
10. Schiffman MH, Brinton LA. The epidemiology of cervical carcinogenesis. Cancer 1995;76:1888–901.
11. Oikawa K, Ohbayashi T, Mimura J, et al. Dioxin suppresses the checkpoint protein, MAD2, by an aryl hydrocarbon receptor-independent pathway. Cancer Res 2001;61: 5707–9.
12. Sok J, Wang XZ, Batchvarova N, Kuroda M, Harding H, Ron D. CHOP-dependent stress-inducible expression of a novel form of carbonic anhydrase VI. Mol Cell Biol 1999;19:495–504.
13. Kuroda M, Ishida T, Takanashi M, Satoh M, Machinami R, Watanabe T. Oncogenic transformation and inhibition of adipocytic conversion of preadipocytes by TLS/FUS-CHOP type II chimeric protein. Am J Pathol 1997;151:735–44.
14. Kuroda M, Horiuchi H, Ono A, Kawakita M, Oka T, Machinami R. Immunohistochemical study on the distribution of sarcoplasmic reticulum calcium ATPase in various human tissues using novel monoclonal antibodies. Virchows Arch A Pathol Anat Histopathol 1992;421:527–32.
15. Oikawa K, Ohbayashi T, Mimura J, et al. Dioxin stimulates synthesis and secretion of IgE-dependent histamine-releasing factor. Biochem Biophys Res Commun 2002; 290:984–7.
16. Kuroda M, Wang X, Sok J, et al. Induction of a secreted protein by the myxoid liposarcoma oncogene. Proc Natl Acad Sci USA 1999;96:5025–30.
17. Nagase T, Seki N, Ishikawa K, et al. Prediction of the coding sequences of unidentified human genes. VI. The coding sequences of 80 new genes (KIAA0201-KIAA0280) deduced by analysis of cDNA clones from cell line KG-1 and brain. DNA Res 1996;3:321–9, 41–54.
18. Hannon GJ. RNA interference. Nature 2002;418:244–51.
19. McManus MT, Sharp PA. Gene silencing in mammals by small interfering RNAs. Nat Rev Genet 2002;3:737–47.
20. Waggoner SE. Cervical cancer. Lancet 2003;361:2217–25.
21. Park TW, Fujiwara H, Wright TC. Molecular biology of cervical cancer and its precursors. Cancer 1995;76:1902–13.
22. Klaes R, Friedrich T, Spitkovsky D, et al. Overexpression of p16^{INK4a} as a specific marker for dysplastic and neoplastic epithelial cells of the cervix uteri. Int J Cancer 2001;92:276–84.

THE JOURNAL OF GENE MEDICINE
J Gene Med 2004; 6: 833–845.
Published online 30 March 2004 in Wiley InterScience (www.interscience.wiley.com). DOI: 10.1002/jgm.583

RESEARCH ARTICLE

Can the life span of human marrow stromal cells be prolonged by bmi-1, E6, E7, and/or telomerase without affecting cardiomyogenic differentiation?

Yukiji Takeda,[1,2,3] Taisuke Mori,[1,2] Hideaki Imabayashi,[1,4] Tohru Kiyono,[5] Satoshi Gojo,[6] Shunichirou Miyoshi,[7] Naoko Hida,[1,2] Makoto Ita,[8] Kaoru Segawa,[9] Satoshi Ogawa,[7] Michiie Sakamoto,[2] Shinobu Nakamura,[3] Akihiro Umezawa[1]*

[1]*Department of Reproductive Biology and Pathology, National Research Institute for Child Health and Development, Tokyo, Japan;* [2]*Department of Pathology, Keio University School of Medicine, Tokyo, Japan;* [3]*Department of General Medicine and Clinical Investigation, Nara Medical University, Nara, Japan;* [4]*Department of Orthopedics, Keio University School of Medicine, Tokyo, Japan;* [5]*Virology Division, National Cancer Center Research Institute, Tokyo, Japan;* [6]*Department of Cardiovascular Surgery, Saitama Medical Center, Kawagoe, Japan;* [7]*Cardiopulmonary Division, Department of Internal Medicine, Keio University School of Medicine, Tokyo, Japan;* [8]*Pharmacia-Keio Research Laboratories, Shinanomachi Research Park, Keio University School of Medicine, Tokyo, Japan;* [9]*Department of Virology, Keio University School of Medicine, Tokyo, Japan*

*Correspondence to: Akihiro Umezawa, Department of Reproductive Biology and Pathology, National Research Institute for Child Health and Development, Okura, Setagaya, Tokyo, 157-8535 Japan. E-mail: umezawa@1985.jukuin.keio.ac.jp

Received: 23 May 2003
Revised: 16 October 2003
Accepted: 27 January 2004

Abstract

Background Cell transplantation has recently been challenged to improve cardiac function of severe heart failure. Human mesenchymal stem cells (hMSCs) are multipotent cells that can be isolated from adult marrow stroma, but because of their limited life span, it is difficult to study them further. To overcome this problem, we attempted to prolong the life span of hMSCs and investigate whether the hMSCs modified with cell-cycle-associated genes can differentiate into cardiomyocytes *in vitro*.

Methods We attempted to prolong the life span of hMSCs by infecting retrovirus encoding bmi-1, human papillomavirus E6 and E7, and/or human telomerase reverse transcriptase genes. To determine whether the hMSCs with an extended life span could differentiate into cardiomyocytes, 5-azacytidine-treated hMSCs were co-cultured with fetal cardiomyocytes *in vitro*.

Result The established hMSCs proliferated over 150 population doublings. On day 3 of co-cultivation, the hMSCs became elongated, like myotubes, began spontaneously beating, and acquired automaticity. Their rhythm clearly differed from that of the surrounding fetal mouse cardiomyocytes. The number of beating cardiomyocytes increased until 3 weeks. hMSCs clearly exhibited differentiated cardiomyocyte phenotypes *in vitro* as revealed by immunocytochemistry, RT-PCR, and action potential recording.

Conclusions The life span of hMSCs was prolonged without interfering with cardiomyogenic differentiation. hMSCs with an extended life span can be used to produce a good experimental model of cardiac cell transplantation and may serve as a highly useful cell source for cardiomyocytic transplantation.

Keywords Bmi-1; marrow stroma; cardiomyocytes; immortalization; papillomavirus; senescence

Introduction

Cell transplantation has recently been attempted to improve cardiac function in severe heart failure. Many types of cells, such as embryonic stem cells [1,2], fetal cardiomyocytes [3–5], myoblasts [6,7], bone marrow hematopoietic cells [8,9], and mesenchymal stem cells (MSCs) [10–12], have been transplanted to functionally restore damaged or diseased tissue in animal models, and mononuclear cells [13–16] or myoblasts [17] have been injected into ischemic hearts clinically.

MSCs can be a useful source of cells for transplantation for several reasons: they have the ability to proliferate and differentiate into mesodermal tissues, including heart, they entail no ethical or immunological problems, and bone marrow aspiration is an established routine procedure. When placed in appropriate *in vitro* and *in vivo* environments, MSCs can give rise to all major mesenchymal tissues, such as bone, cartilage, muscle, and adipose tissue [18]. Murine MSCs can also differentiate into cardiomyocytes and start to beat synchronously *in vitro* [19], and direct injection of murine MSCs into the heart has been shown to be feasible in murine models of ischemic heart disease and normal mouse heart. Thus far, only endothelial cells have been shown to exhibit '*in vitro* cardiomyogenesis' in humans [20].

Large numbers of cells must be injected into damaged sites in ischemic heart disease to restore cardiac function in humans, and cells need to be injected into the entire heart in cardiomyopathy. Until now, however, there have been no reports of a sufficient number of differentiated human cardiomyocytes ever having been obtained to restore the function of a failing heart. One of the reasons for this is that the life span of human cells *in vitro* is limited. Human cells reach senescence or stop cell growth after a limited number of cell replications [21], and the average number of hMSC population doublings (PDs) has been found to be 38 [22], implying that it would be difficult to obtain enough cells to restore the function of a failing human heart.

To resolve these problems and to establish a model of cell therapy of the failing heart, we attempted to prolong the life span of hMSCs by using the system to infect retrovirus encoding bmi-1, human telomerase reverse transcriptase (TERT), and human papillomavirus E6 and E7 genes. Both Rb/p16INK4a inactivation with E7 and telomerase activation with E6 are required to extend the life span of human epithelial cells [23]. bmi-1, a c-myc cooperating oncogene in murine lymphomas, reduces expression of p16INK4a, stimulates cell proliferation [24], and is required for maintenance of self-renewing hematopoietic stem cells [25,26]. This method was highly efficient in extending the life span of hMSCs. In the present study we investigated whether hMSCs with an extended life span have the ability to differentiate into cardiomyocytes *in vitro*.

Materials and methods

Isolation and cell culture of hMSCs

After obtaining signed informed consent, bone marrow cells were harvested from a 91-year-old human female donor with the approval of the Ethics Committee of Keio University School of Medicine (Tokyo). Cells were resuspended in bone marrow stromal cell culture medium (10% fetal bovine serum in Dulbecco's modified Eagle's medium containing 4.5 g/l glucose [DMEM-HG]) with antibiotic/antimycotic supplements (Gibco), and cultures were maintained at 37 °C in a humidified atmosphere containing 95% air and 5% CO_2. When the cultures reached subconfluence, the cells were harvested with 0.25% trypsin and 1 mM EDTA, and replated with one half of the harvested cells. After a series of passages, the attached marrow stromal cells were devoid of hematopoietic cells. Several bone marrow stromal cell strains were then generated by the limiting-dilution method, and one of them was designated H4-1. The H4-1 cells were cultured in MSC growth medium (MSCGM) at 37 °C in a humidified atmosphere containing 95% air and 5% CO_2.

Preparation and infection of recombinant retroviruses

The full-length human bmi-1 cDNA was cloned by RT-PCR using RNA extracted from K562 cells. Thermoscript reverse transcriptase (Invitrogen) and KOD polymerase (TOYOBO, Japan) were used for the RT and PCR reactions, respectively. The forward primer, 5'-ACGCGTCGACCGCCATGCATCGAACAACGAGAAT-3', and reverse primer, 5'-CGGATCCTCAACCAGAAGAAGTTGCTG-3', were designed to obtain the coding sequence of human bmi-1 flanked by the *SalI* site (underlined) and the Kozak consensus sequence at the 5'-end and the *Bam*HI site (underlined) at the 3'-end. The *SalI-Bam*HI segment of the PCR product was cloned between the *Xho*I and *Bgl*II sites of pCLXSN to generate pCLXSN-bmi1. The coding sequence of the cDNA was confirmed to be identical to the published sequence (NCBI ACC# NM_005 180.4). Construction of pCLXSH-hTERT has been described previously [27]. The gateway system (Invitrogen) was used to subclone a deletion mutant of HPV16 E6 (16E6SDD151) that lacked transforming activity to 3Y1 cells [28] into pCMSCVpuro. pCMSCVpuro comprises the CMV/LTR fusion promoter, the packaging signal Psi, and the multicloning sequence from pCLXSN (Imgenex Corp., San Diego, CA, USA) followed by the PGK-puro cassette and the 3' long terminal repeat of murine embryonic stem cell virus from pMSCVpuro (Clontech). The destination vector pCMSCVpuro-DEST was constructed by inserting a modified cassette containing attR sites and ccdB (Invitrogen) between the *Eco*RI and *Bgl*II sites of pCMSCVpuro. 16E6SDD151 was first recombined into pDONR201 by BP reaction, and then into the destination vector by LR reaction according to the manufacturer's instructions (Invitrogen) to generate pCMSCVpuro-16E6SDD151. Production of recombinant retroviruses has been described previously [29,30]. Briefly, the retroviral vector together with the packaging construct, pCL-10A1, was transfected into 293T cells, and the culture fluid was harvested 48–72 h post-transfection. The preparation of the LXSN-16E7 retrovirus and the infection protocols have been described previously [31], except that FLYA13 [32] was used as the packaging cell line instead of PG13. The titers of the recombinant viruses were greater than 5×10^5 drug-resistant colony-forming units per milliliter on HeLa

cells, and 1 ml of the culture fluid was added to the cells in the presence of polybrene (8 μg/ml). Following inoculation with the viruses, hMSCs were grown in the presence of G418 (100 μg/ml), hygromycin B (50 μg/ml), or puromycin (1 μg/ml), and a polyclonal drug-resistant cell line was established and further analyzed. To achieve combinations of retroviral infections, cells were sequentially transduced with LXSN-E7 or LXSN-bmi-1, and LXSH-hTERT, and then MSCVpuro-16E6SDD151, if indicated, and selected with G418, hygromycin B, and puromycin, respectively. The stably transduced cells with an expanded life span were designated UBT-5, UBET-7, UEET-1, UEET-11, and UET-13.

Flow cytometric analysis

Cells were detached and stained for 30 min at 4 °C with primary antibodies and immunofluorescent secondary antibodies. After washing, the cells were analyzed on an EPICS ALTRA analyzer (Beckman Coulter). Antibodies (anti-human CD13, CD14, CD24, CD29, CD31, CD34, CD44, CD45, CD50, CD54, CD55, CD59, CD90, CD105, CD117, CD133, CD140a, CD166, Flk-1) were purchased from Beckman Coulter, Immunotech, Cytotech, and Pharmingen Pharmaceutical, Inc.

Introduction of the GFP and β-galactosidase genes

Recombinant adenovirus expressing β-galactosidase and the green fluorescent protein (GFP) was prepared as described [33]. Cells were infected with these viruses at 10 plaque-forming units/cell. hMSCs were examined cytochemically *in vitro* for expression of the β-galactosidase gene and by fluorescent confocal microscopy for expression of the GFP gene. By 7 days post-infection nearly all the cells expressed β-galactosidase and GFP.

Preparation of murine fetal cardiomyocytes

Fetal cardiomyocytes were obtained from the hearts of day 14 mouse fetuses. Hearts were minced with scissors and washed with phosphate-buffered saline (PBS), and the minced hearts were incubated in PBS with 0.05% trypsin and 0.25 mM EDTA for 5 min at 37 °C. After adding DMEM supplemented with 10% fetal bovine serum (FBS), the cardiomyocytes were centrifuged at 1000 rpm for 5 min. The pellet was then resuspended in 10 ml DMEM with 10% FBS and incubated on glass dishes for 1 h to separate the cardiomyocytes from fibroblasts. The floating cardiomyocytes were collected and replated at $1 \times 10^5/cm^2$.

hMSC and murine fetal cardiomyocyte co-culture system

Human MSCs were plated on dishes at $5 \times 10^4/cm^2$, and infected with EGFP-expressing adenovirus on the next day. The supernatant was then removed, and the cells were cultured for 2 days in DMEM supplemented with 10% FBS. The cells were then exposed to 10 μM of 5-azacytidine for 24 h to induce cell differentiation. The 5-azacytidine-treated hMSCs were harvested with 0.25% trypsin and 1 mM EDTA and overlaid onto the fetal cardiomyocytes at $5 \times 10^3/cm^2$. The morphology of the beating hMSCs was evaluated under a fluorescent microscope.

RT-PCR

Total RNA was prepared from co-cultured hMSCs and mouse heart with Isogen (Nippon Gene). Human cardiac RNA was purchased (Clontech). RNA for RT-PCR was converted to cDNA with a first-strand cDNA synthesis kit (Amersham Pharmacia Biotec) according to the manufacturer's recommendations. RT-PCR of the bmi-1, E6, E7, TERT, myosin light chain-2a (MLC-2a), Nkx2.5, and human atrial natriuretic peptide (hANP) genes was performed, and the PCR primers used are listed in Table 1. RT-PCR was performed with PCR primers that can amplify human but not mouse genes. PCR primers of 18S used as a positive control react with both human and murine genes. PCR was performed with TaKaRa Z-Taq (Takara Shuzo Co., Ltd) for 30 cycles, with each cycle consisting of 98 °C for 5 s, 68 °C or 60 °C for 1 s, and 72 °C for 10 s, with an additional 30-s incubation at 72 °C after completion of the final cycle.

Action potential recording and microinjection of dye

An inverted microscope (IX-70, Olympus, Tokyo, Japan) with a fluorescence filter (U-MNIBA2, Olympus) was used for action potential (AP) recording. The microscope was equipped with a recording chamber and a noise-free heating plate (Microwarm Plate, Kitazato Supply, Fujinomiya, Shizuoka, Japan). A 10 mmol/l volume of HEPES was added to the culture medium to stabilize the pH of the perfusate at 7.5–7.6. Standard glass microelectrodes having a DC resistance of 25–35 MΩ when filled with pipette solution were used. Alexa 568 compound was dissolved to a concentration of 0.5 mmol/l in 2 mol/l of KCl solution in order to completely dissolve the Alexa 568 in the pipette solution. The electrodes were positioned with a motor-driven micromanipulator (PCS-5000, Burleigh Instruments, Inc., New York, USA) under optical control. Spontaneously beating GFP-positive cells were selected as targets, and, after the APs of the targeted cells had been recorded, the dye was injected by iontophoresis (−7 nA for 30–60 s). The extent

Table 1. PCR primers used in this study

Gene product	Primer (sense)	Primer (anti-sense)	Annealing temperature (°C)	Product size (bp)
Bmi-1	TCATCCTTCTGCTGATGCTG	GCATCACAGTCATTGCTGCT	60	220
E6	GACCCAGAAAGTTACCACAG	GCAACAAGACATACATCGAC	60	397
E7	ATGACAGCTCAGAGGAGGAG	TCCTAGTGTGCCCATTAACAG	60	178
TERT	CGGAAGAGTGTCTGGAGCAA	GGATGAAGCGGAGTCTGGA	60	144
MLC-2a				
1st	TCGTGATGGCATCATCTGCAAGG	ACAGAGTTTATTGAGGTGCCCC	60	429
2nd	AAGGTGAGTGTCCCAGAGG	ATGGGTGTCAGGGCGAACATC	60	259
NkX2.5				
1st	CTTCAAGCCAGAGGCCTACG	CCGCCTCTGTCTTCTCCAGC	60	233
2nd	CTTCACCGGCCAAGTGTGCGTC	CCGCCTCTGTCTTCTCCAGC	60	152
hANP				
1st	GAACCAGAGGGGAGAGACAGAG	CCCTCAGCTTGCTTTTTAGGAG	60	406
2nd	GTCAGACCAGAGCTAATCCC	ACCTCCATCTCTCTGGGCTG	68	223
18S	GTGGAGCGATTTGTCTGGTT	CGCTGAGCCAGTCAGTGTAG	60	200

of dye transfer was monitored under a fluorescence microscope, and digital images were recorded with a digital photo camera (D100; Nikon, Tokyo, Japan) mounted on the microscope with a fluorescence filter (U-MWIG2; Olympus). The recording pipette was connected to a patch-clamp amplifier (Axopatch 200B; Axon Instruments), and the signal was low-pass filtered at 2 kHz and digitized with an A/D converter with sampling frequency of 10 kHz (Digidata 1322A; Axon Instruments) connected to a computer with Pentium4. Signals were monitored, recorded as electric files, and analyzed offline with pCLAMP 8.2 software (Axon Instruments). The rhythm was considered regular if the maximum beating rate minus the minimum beating rate divided by the max beating rate was <0.4.

Immunohistochemistry

The hMSCs co-cultured with fetal cardiomyocytes *in vitro* were fixed with 4% PFA and stained with anti-β2microglobulin antibody at 1 : 1000, mouse monoclonal antibody against troponin I (Hytest, Euro, Finland) at 1 : 200, anti-desmin antibody at 1 : 100, and anti-β-galactosidase antibody (Chemicon) at 1 : 500. hMSCs expressing GFP were fixed with 4% PFA.

Results

Establishment of hMSCs with an extended life span

H4-1 cells were obtained from primary culture by limiting dilution (Figure 1A). The cells proliferated for a limited number of passages and then underwent senescence, as evidenced by the cells assuming a broad and flattened shape (Figures 1B and 1C). To extend the life span of H4-1 cells, and obtain a large number of cells for cardiac transplantation, four different types of cells were obtained by transferring combinations of bmi-1, E6, E7, and/or TERT genes. Cells transduced with bmi-1 and TERT were designated UBT-5 cells; cells transduced with bmi-1, E6, and TERT were named UBET-7 cells; cells transduced with E7 and TERT were designated UET-13 cells; and cells transduced with E6, E7, and TERT were named UEET-1 and UEET-11 cells (Figures 1D, 1E, and 1F). To simplify nomenclature and avoid confusion, we use the name UEET-1 to refer to cells transduced with E6, E7, and TERT although they have recently been reported as ThMSC1 [29]. The cells were subcloned after each gene transfer, and thus were clonal. The UEET-1 cells were spindle-shaped, and longer than the parental H4-1 cells (Figures 1B, 1D, and 1E). Characteristics of cells with a prolonged life span were investigated. UEET-11 and UET-13 proliferated more than 150 PDs in 400 days, and UBET-7 and UBT-5 proliferated more than 50 PDs in 400 days, while H4-1 stopped dividing at 38 PDs (approximately 200 days). The growth rates of UEET-11 and UET-13 were higher than those of UBT-5 and UBET-7. Chromosome analysis revealed parental H4-1 and UET-13 to exhibit normal karyotypes, while the other cells transduced with E6 and E7 showed chromosome aberrations at low frequencies (data not shown). The transduced cells did not generate tumors, at least for the first 60 days after subcutaneous transplantation into immunodeficient mice.

Surface analysis of hMSCs

Surface markers of the UEET-1, UEET-11, UBT-5, UBET-7, and UET-13 cells were evaluated by flow cytometric analysis. The results showed that all of the MSCs were positive for CD13, CD29 (integrin β1), CD44 (Pgp-1/ly-24), CD55, CD59, CD90 (Thy-1), CD105 (endoglin), CD133, CD140a (PDGFRα or PDGFR2), and CD166 (ALCAM), and negative for CD14 (a marker for macrophage and dendritic cells), CD24, CD31 (PECAM-1), CD34, CD45 (leukocyte common antigen), CD50 (ICAM-3), CD54, CD117 (c-kit), and Flk-1 (Figure 2). Parental H4-1 cells had the same pattern of surface markers as UEET-1, UEET-11, UBT-5, and UBET-7 cells, implying that the surface markers were not influenced by

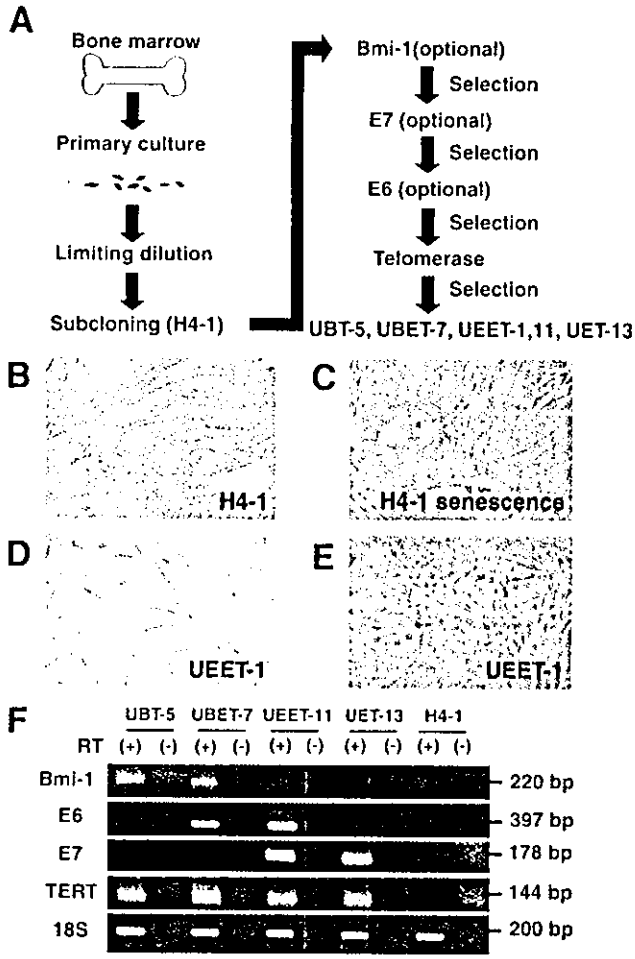

Figure 1. Experimental scheme. (A) Bone marrow stromal cells were obtained from a human donor and subcloned by limiting dilution. One of the cells isolated was designated H4-1 cells, and they were transduced with E6, E7, TERT, or bmi-1 genes to extend their life span. The combinations of genes transferred were: (1) bmi-1 and TERT; (2) bmi-1, E7, and TERT; (3) E7 and TERT; and (4) E6, E7, and TERT. (B) H4-1 cells in the growth phase. (C) H4-1 cells at senescence. The cells showed a broad and flattened shape. (D) H4-1 cells after transfer of E6, E7, and TERT genes were designated UEET-1 cells. (E) UEET-1 cells at confluence. Original magnification, B–E: ×100. (F) The gene expression in each cell line was analyzed using RT-PCR

the exogeneously expressed bmi-1, E6, E7, and/or TERT genes.

Cardiomyogenic differentiation of hMSCs and stably transduced hMSCs

To determine whether H4-1 cells could be induced to undergo cardiomyogenic differentiation, the cells were exposed to 10 μM of 5-azacytidine for 24 h as previously reported in murine stromal cells [19]. All of the transduced hMSCs did not exhibit spontaneous beating despite continuous culturing for up to 3 months. Immunocytochemical analysis revealed the presence of desmin, a myocytic marker, in the hMSCs with an extended life span, i.e., UBT-5 cells and UBET-7 cells (Figure 3A). However, all cells tested were negative for the cardiomyocyte marker troponin-I (Figure 3B).

We employed a co-culture system with fetal cardiomyocytes to induce cardiac differentiation (Figure 4), since *in vitro* simulation of the heart by the environment has been shown to be an efficient means of induced differentiation of human endothelial progenitor cells and murine marrow stromal cells [20,34]. After exposing GFP-labeled UBT-5, UBET-7, UEET-11, and UET-13 cells to 10 μM of 5-azacytidine for 24 h, these cells were co-cultured with fetal cardiomyocytes. On day 3 after the start of co-cultivation, a few GFP-positive UBET-7 cells started to contract (Figure 5A). The contraction was stronger when beating cells were clustered than when scattered (Figure 5B). On day 7, the beating of the UBET-7 cells was synchronous with that of adjacent cells and was independent of that of the surrounding murine cardiomyocytes (Figures 5C and 5D). Repetition of these experiments confirmed the results to be reproducible, and the percentages of UBT-5, UBET-7, UEET-11, and UET-13 cells that underwent cardiomyogenic differentiation were almost the same, implying that cardiomyogenic differentiation is independent of the genes transferred. The number of beating cells increased for up to 3–4 weeks, when the fetal cardiomyocytes spontaneously detached from the dishes (Figure 5E). UBET-7 cells not treated with 5-azacytidine were co-cultured with fetal cardiomyocytes to determine whether environmental factors alone can induce cardiac differentiation, but fewer beating cells were observed (Figure 5F). No significant difference was detected in the number of differentiated cells between parental H4-1 and UBET-7 (Figure 5G).

Expression of cardiomyocyte-specific genes and proteins and the action potential of differentiated hMSCs

We analyzed the co-cultured UBET-7 cells in terms of gene expression and by immunocytochemistry and electrical recording. RT-PCR was performed with primers that react with human cardiomyocyte-specific genes but not with murine orthologues. Differentiated UBET-7 cells expressed MLC-2a, hANP, and the cardiomyocyte-specific transcription factor, Nkx2.5/Csx (Figure 6). Sequence analysis revealed that the cDNAs matched the sequences of the human MLC-2a, hANP, and Nkx2.5/Csx genes.

Action potentials were recorded from spontaneously beating cells. Alexa 568 was injected into cells via a recording microelectrode to stain the cells and confirm that the action potential was generated by GFP-positive UBET-7 cells (Figures 7A and 7B). Since the dye did not diffuse into the murine cardiomyocytes, there were no tight cell-to-cell heterologous connections, i.e., gap junctions. In some experiments, Alexa 568 diffused into the GFP-positive satellite UBET-7 cells, suggesting that a homologous cell-to-cell connection had been established at least 1 week after co-cultivation. The measured parameters of the recorded action potential were averaged

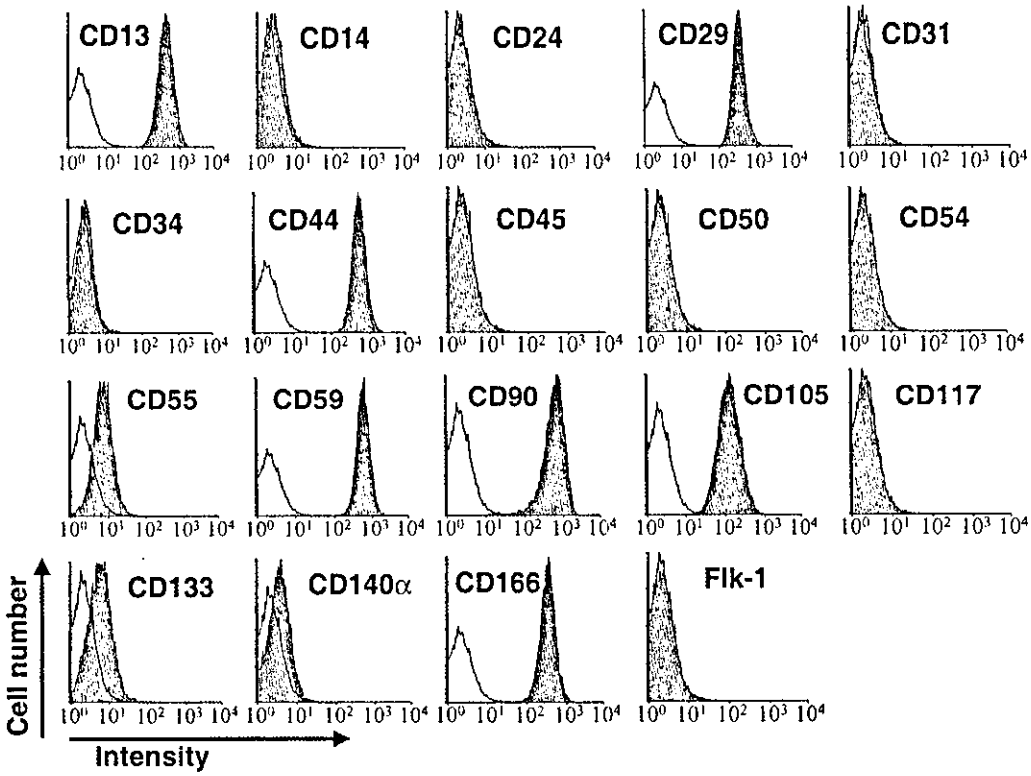

Figure 2. Flow cytometric analysis of UEET-1 cells. UEET-1 cells were labeled with FITC-coupled antibodies against CD13, CD14, CD24, CD29, CD31, CD34, CD44, CD45, CD50, CD54, CD55, CD59, CD90, CD105, CD117, CD133, CD140a, CD166, and Flk-1 and analyzed with an EPICS ALTRA analyzer

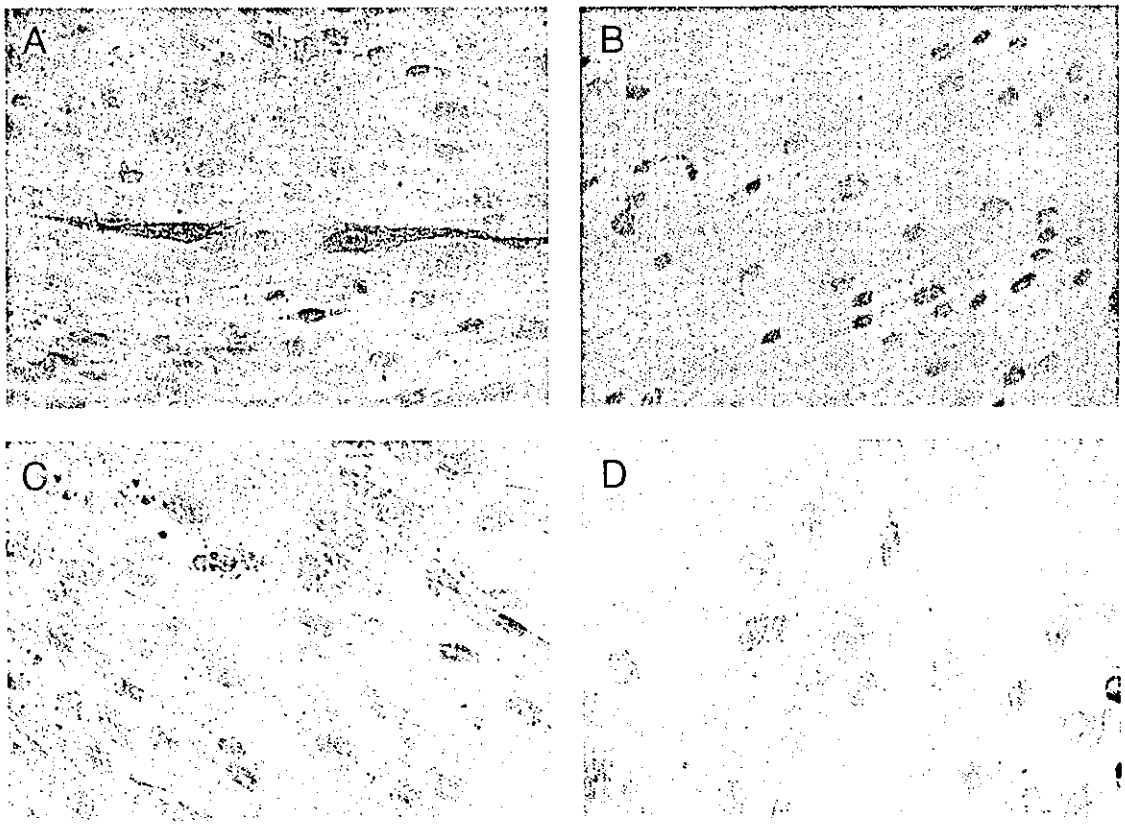

Figure 3. Immunostaining of hMSCs with anti-desmin and anti-troponin-I antibodies after exposure to 5-azacytidine. UBET-7 cells were exposed to 10 μM of 5-azacytidine for 24 h and stained for desmin (A) and cardiac troponin I (B). UBET-7 cells not treated with 5-azacytidine were also stained for desmin (C) and cardiac troponin I (D). Original magnification: ×400

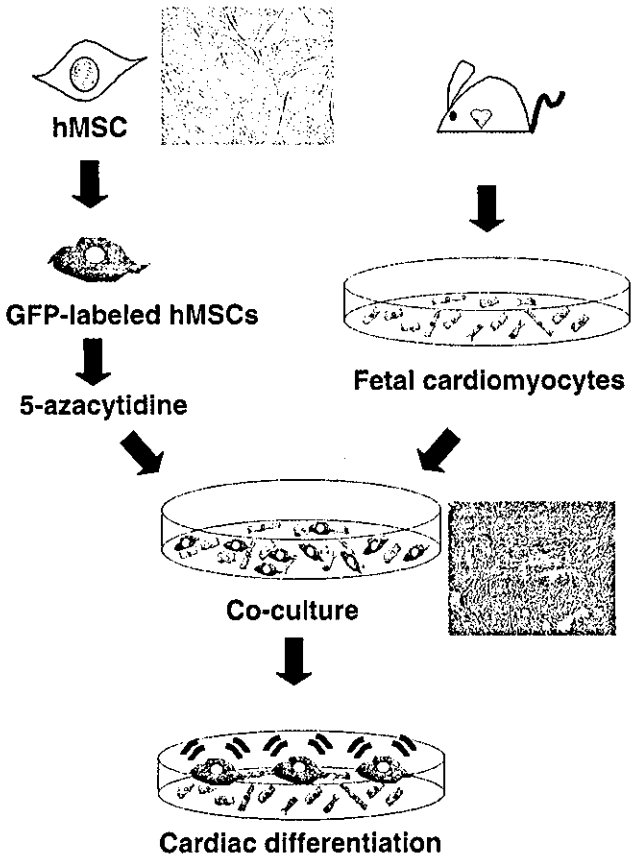

Figure 4. Scheme of the co-culture system. hMSCs infected with adenoviruses carrying the GFP gene were treated with 10 μM of 5-azacytidine for 24 h. hMSCs expressing GFP were then co-cultured with murine fetal cardiomyocytes. hMSCs began beating spontaneously after 7 days of co-culture

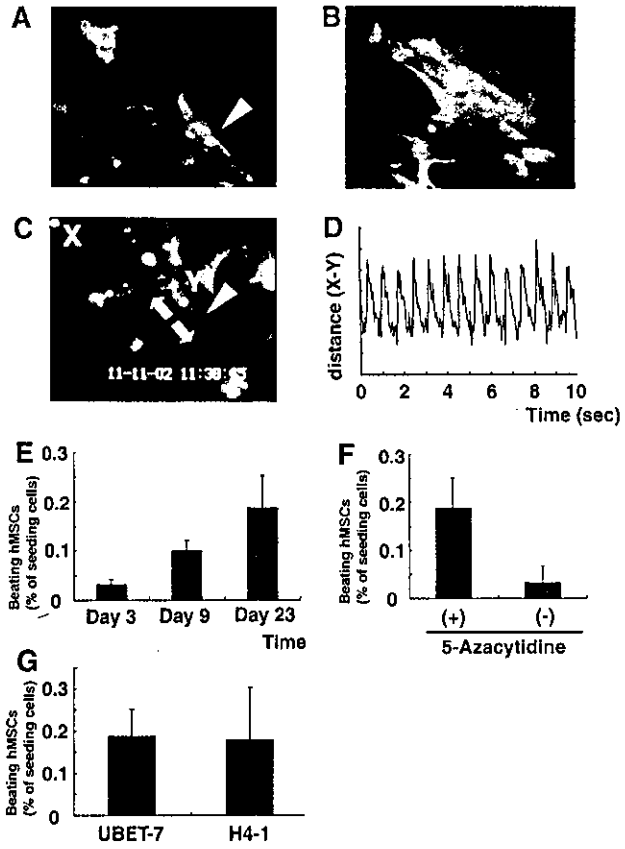

Figure 5. Beating of hMSCs in the *in vitro* co-culture system. (A) 5-Azacytidine-treated GFP-positive UBET-7 cells were co-cultured with murine fetal cardiomyocytes (http://1985.jukuin.keio.ac.jp/umeza/jgm/ubet7). The white arrowhead is pointing to some beating UBET-7 cells whose rhythm was different from that of the fetal cardiomyocytes. (B) More UBET-7 cells tended to contract in areas where they were clustered than in areas where they were scattered. (C) Beating UBET-7 cells were videotaped at 30 flames/s and their contractions were analyzed. Point X in this view was fixed, and point Y was used as a reference point on the differentiated UBET-7 cell (arrowhead). Arrows point in the direction of contraction, and point Y moved with each contraction. Original magnification, A–C: ×150. (D) The distances between points X and Y were measured for a 10-s period and plotted on the graph. The UBET-7 cells contracted regularly at 84 beats/min. (E) The ratio of the number of beating UBET-7 cells to the number of the cells seeded increased for 3 weeks. (F) On day 23, the ratio was higher in the cells exposed to 5-azacytidine than in the cells not exposed to 5-azacytidine. (G) Parental H4-1 was compared with UBET-7 in terms of the number of beating cells

(Table 2). The duration of the action potentials of the UBET-7 cells was extremely long, and they were therefore concluded to be action potentials of cardiomyocytes, not of smooth muscle, nerve cells, or skeletal muscle. Time-course analysis of the action potentials revealed shortening of their duration, a gain in amplitude, and stabilization and organization of the spontaneous beating rhythm. Representative action potential recordings are shown in Figures 7C and 7D. The rhythm of some (33%) of the UBET-7 cells was still disorganized at 1 week (Figure 7C), whereas the rhythm of the UBET-7 cells (100%) had become regular and had stabilized at 3 weeks (Figure 7D).

Immunohistochemistry revealed that UBET-7 cells expressing human β2microglobulin and GFP stained positive for desmin (Figures 8A–8C) and cardiac troponin I (Figures 8D–8F) on day 14. Clear striations were observed in the differentiated UBET-7 cells (Figure 8H).

Absence of cell fusion between hMSCs and murine fetal cardiomyocytes

To determine whether the beating cells had fused with the fetal cardiomyocytes, GFP-expressing hMSCs were co-cultured with fetal cardiomyocytes labeled with β-galactosidase. On day 7, when almost 100% of the cardiomyocytes were labeled with β-galactosidase, and almost 100% of the co-cultured-hMSCs expressed GFP, none of the cells were double-stained for GFP and β-galactosidase (Figures 9A–9D). This observation indicates that the cardiomyogenic differentiation of hMSCs is not attributable to cell fusion on day 7.

Discussion

This study was conducted to determine whether prolongation of cell life span by cell-cycle-associated molecules

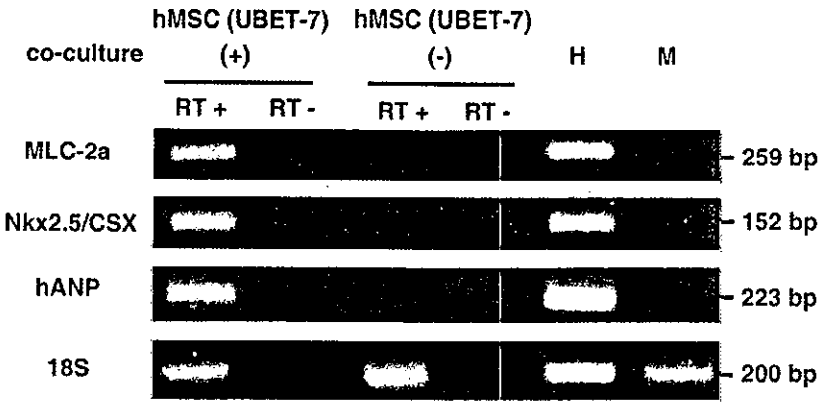

Figure 6. Expression of cardiomyocyte-specific genes in differentiated hMSCs (UBET-7). RT-PCR was performed with PCR primers that react with human genes encoding cardiac proteins (MLC-2a, Nkx2.5, and hANP) but do not with the murine genes. Only the 18S PCR primer used as a positive control reacted with the human and murine genes. Human heart (H) and mouse heart (M) were used as a positive control and negative control, respectively. The human cardiac genes, MLC-2a, Nkx2.5/csx and hANP, were expressed in the co-culturing system, but were not expressed in the undifferentiated state (without feeder cells)

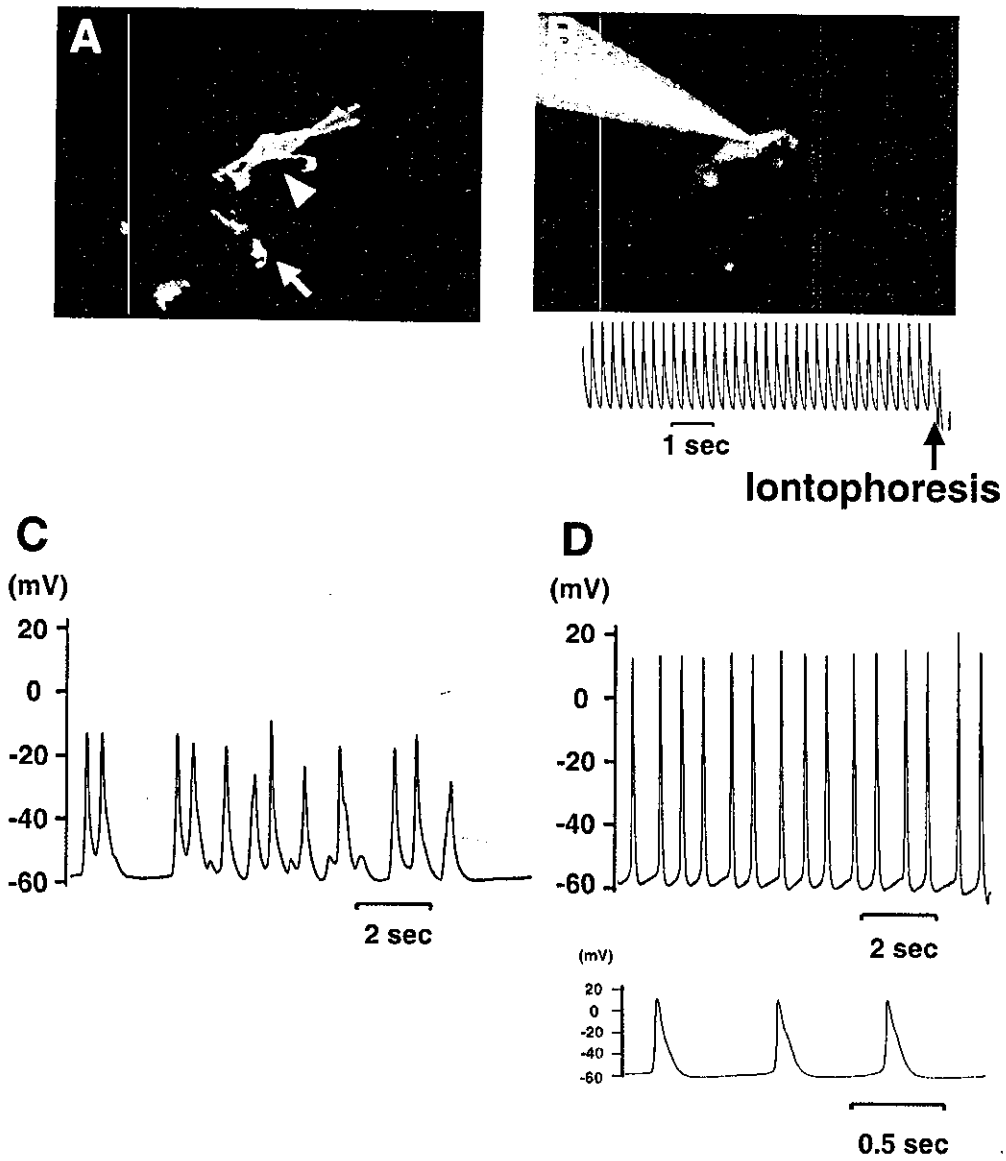

Figure 7. Action potentials of beating hMSCs. GFP-labeled UBET-7 cells (A) were injected with Alexa 568 solution (B) by iontophoresis through a microelectrode. The injected UBET-7 cell and neighboring beating UBET-7 cell are indicated by arrowhead and arrow, respectively. The action potential was recorded (B, lower panel). Some of the rhythms recorded at 1 week of co-cultivation were irregular (C), but the rhythm became regular at 3 weeks (D); top: large scale (2 s), bottom: small scale (0.5 s). Original magnification, A, B: ×400

Table 2. Action potential parameters in human mesenchymal stem cell derived cardiomyocytes

Time of co-culture	n	Ratio of regular rate	Beating rate (beats/min)	MDP (mV)	Amplitude (mV)	APD_{90} (ms)
1 week	12	67%	70.6 ± 12.8	−49.9 ± 1.6	47.2 ± 2.9	345.8 ± 21.4
2 weeks	9	67%	65.9 ± 12.7	−50.3 ± 2.3	60.2 ± 4.5	169.7 ± 13.8
3 weeks	9	100%	68.2 ± 12.1	−45.1 ± 1.4	63.7 ± 3.0	163.4 ± 16.5

The values are shown as mean ± S.E. The ratio of regular rate: regular beating rhythm/irregular beating rhythm. MDP: maximum diastolic potential. APD: action potential duration.

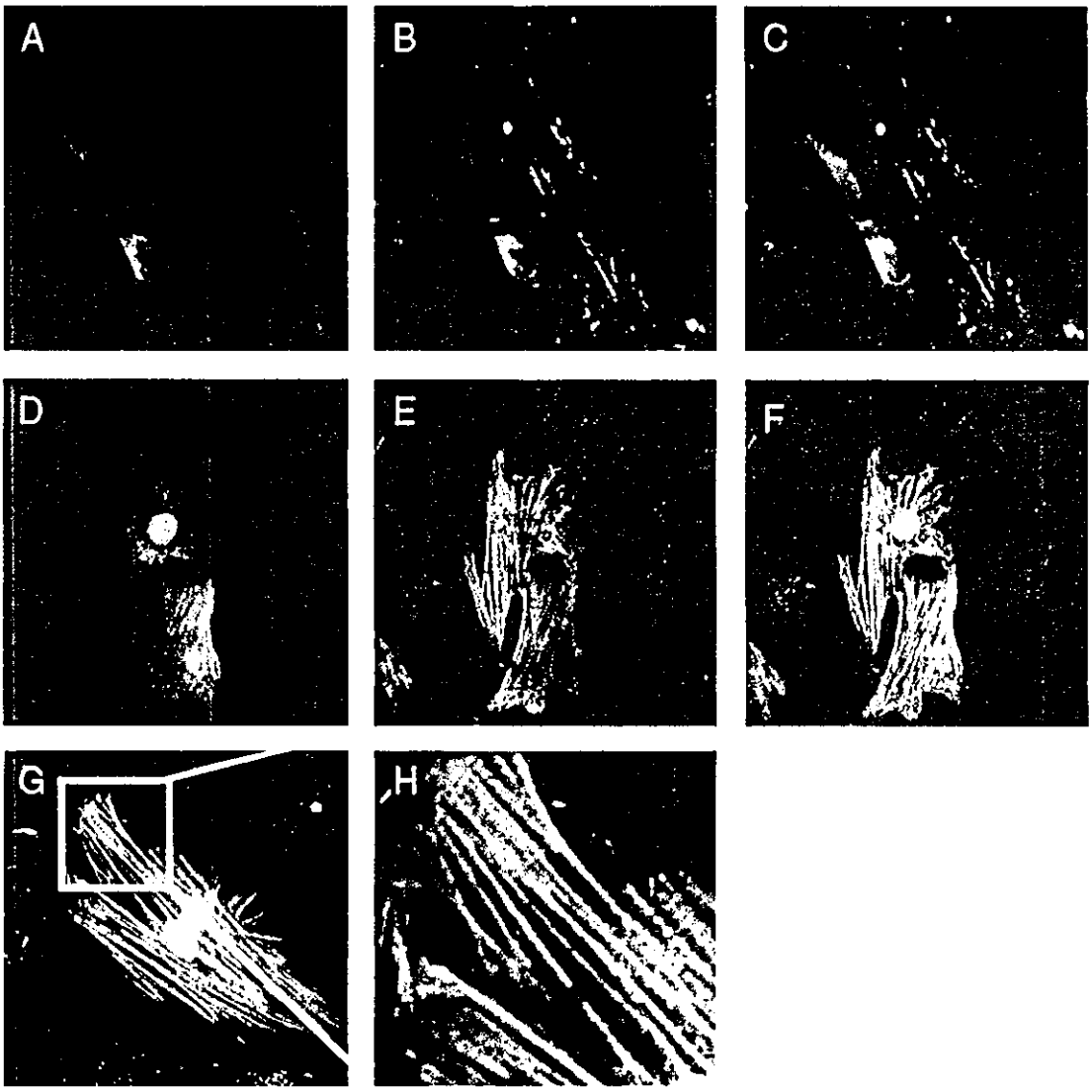

Figure 8. Immunocytochemistry of differentiated hMSCs with anti-desmin and anti-troponin-I antibodies. UBET-7 cells were co-cultured with cardiomyocytes. UBET-7 cells were analyzed for myogenic and cardiac differentiation by immunohistochemistry with desmin and cardiac troponin-I, respectively. Co-cultured UBET-7 cells were stained with anti-β2microglobulin antibody (A) and anti-desmin antibody (B). A superimposed image ('Merge') of A and B is shown in C. GFP-expressing UBET-7 cells (D) were stained with anti-troponin-I antibody (E). 'Merge' is shown in F. A differentiated UBET-7 cell is shown at higher magnification (G). The differentiated UBET-7 cells have striations in their cytoplasm (H). Original magnification, A–G: ×600, H: ×2000

would predominate over cardiomyogenic differentiation of marrow stromal cells *in vitro*. The primary findings of the present study were: (1) the life span of hMSCs was extended by bmi-1, E6, E7, and TERT; (2) hMSCs exposed to 5-azacytidine and cultured with fetal cardiomyocytes underwent cardiomyogenic differentiation as manifested by their morphology, gene expression, and electrophysiology, and started to beat spontaneously (automaticity); and (3) cardiomyogenic differentiation of the hMSCs was not attributable to cell fusion.

MSCs are pluripotent cells capable of differentiating into many cell types, such as neurons [35], myocytes, cardiomyocytes, chondrocytes, and adipocytes [36]. Multipotent adult progenitor cells (MAPCs) have recently

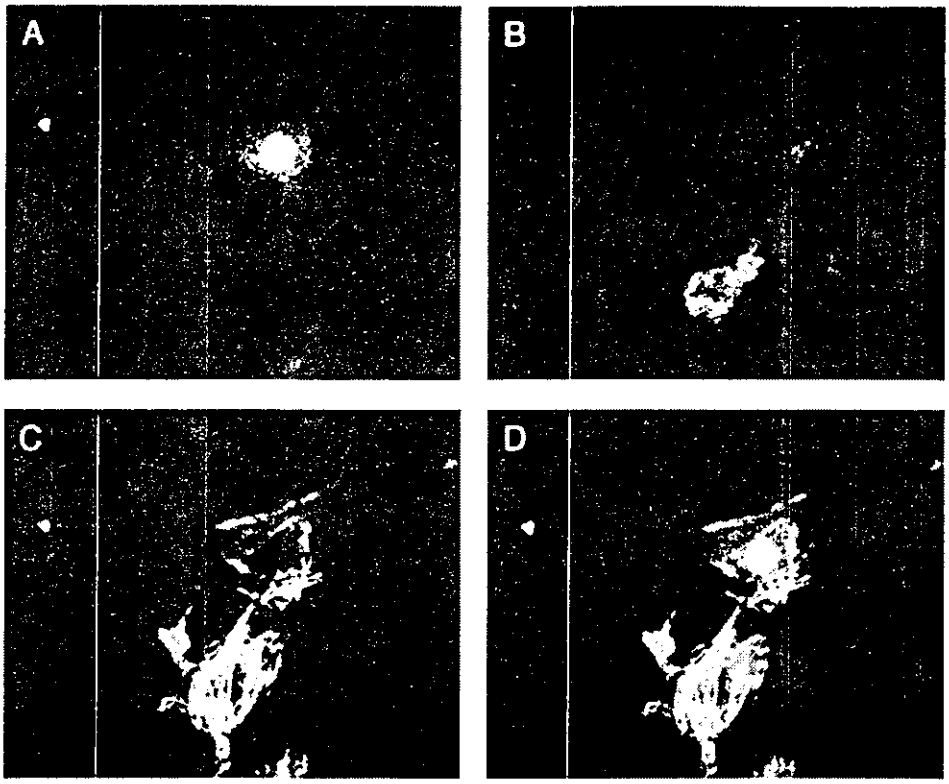

Figure 9. Cardiomyogenic differentiation of hMSCs is not due to cell fusion. We labeled UBET-7 cells with GFP (A) and murine cardiomyocytes with β-galactosidase (B). Cells were tested for the presence of β-galactosidase immunocytochemically (B, Cy5). Differentiation of UBET-7 cells was determined with anti-troponin I antibody (C, Rhodamine). 'Merge' of A, B, and C is shown in D. The differentiated GFP-expressing UBET-7 cells had not fused with murine feeder cells labeled with β-galactosidase. Original magnification: ×600

been shown to differentiate, at single cell level, not only into mesenchymal cells, but also into cells with characteristics of visceral mesoderm, neuroectoderm, and endoderm [37]. MAPCs have the ability to proliferate extensively without any clear evidence of senescence or loss of differentiation potential, and they are thought to be extremely similar to embryonic stem (ES) cells. MSCs and MAPCs also have the advantages of the absence of ethical and immunological problems, and undesired differentiation is infrequent. Thus they are one of the most promising sources of cells for cell therapy.

However, there are two major problems with hMSCs: (1) a large enough number of cells to regenerate tissue by cell transplantation is difficult to obtain, and (2) detailed investigation has been limited by their finite life span. A system that allows human cells to escape senescence by using cell-cycle-associated molecules may be used to obtain sources of cell therapy and to overcome these problems and establish a good model of cell transplantation to the failing heart [23,38]. Both inactivation of the Rb/p16INK4a pathway and activation of telomerase are required for immortalization of human epithelial cells such as mammary epithelial cells and skin keratinocytes. Human papillomavirus E7 can inactivate pRb, and bmi-1 can repress p16INK4a expression. Inactivation of the p53 pathway is also beneficial, even if not essential, to extension of the life span [39]. Based on the above notion, we transferred E7 or bmi-1 plus hTERT in combination with or without E6 into hMSCs and obtained several hMSC strains with an extended life span: UEET-1, UBT-5, UBET-7, UEET-11, and UET-13 cells. The cells with the extended life span continued growing *in vitro* for over 150 PDs, and their differentiation potential was maintained. Transfer of TERT alone was insufficient to prolong the life span of hMSCs in the present study, despite TERT having been reported to extend the life span of cells beyond senescence without affecting their differentiation ability [40]. The characteristics of the cells with an extended life span were unchanged after transfer of bmi-1, E6, E7, and TERT genes, and this finding is consistent with flow cytometric analysis showing that the surface markers of H4-1 cells and stably transduced cells (UEET-1, UBT-5, UBET-7, UEET-11, and UET-13) are identical [29].

In this study, we used the demethylating agent 5-azacytidine as an inducer, the same as in murine marrow stromal cells [19], and clearly showed that co-cultivation with fetal cardiomyocytes is necessary to induce cardiomyogenic differentiation which could be further enhanced by pretreatment of cells with 5-azacytidine. 5-Azacytidine is a cytosine analog that has a remarkable effect on transdifferentiation of cells and has been shown to induce differentiation of mesenchymal cells into cardiomyocytes, skeletal myocytes, adipocytes, and chondrocytes [19,41]. The effect of this low-molecular substance is not surprising, since 5-azacytidine

is incorporated into DNA and has been shown to cause extensive demethylation. The demethylation is attributable to covalent binding of DNA methyltransferase to 5-azacytidine in the DNA [42], with the subsequent reduction of enzyme activity in cells resulting in dilution-out and random loss of methylation at many sites in the genome. This may in turn account for the reactivation of cardiomyogenic 'master' genes, such as MEF-2C, GATA4, dHAND, and Nkx2.5/Csx, leading to stochastic transdifferentiation of MSCs into cardiomyocytes. Use of 5-azacytidine is beneficial, but since it may have drawbacks, i.e., gene activation leading to oncogenesis and undesired differentiation, care must be exercised before using it to simply induce cells to differentiate into target phenotype(s) because of its stochastic nature.

Thus, it may be necessary to find alternative humoral factors essential for cardiomyogenic differentiation to prepare cells for cell therapy in humans. In addition to demethylating agents, environmental factors promote cardiomyocyte differentiation. A co-culture system has recently been used to induce cardiac differentiation, and human endothelial progenitor cells have been found to transdifferentiate into cardiomyocytes with this system [20]. Murine MSCs have been shown to differentiate into a cardiomyogenic lineage [43], but to our knowledge the present study is the first to report spontaneous beating by human MSCs and exhibition of *'in vitro'* automaticity without cell fusion. These results simply imply that MSCs may have the ability to transdifferentiate into cardiomyocytes in response to demethylation of the genome, in addition to environmental factors.

Co-cultivation makes it difficult to investigate two different types of cells in detail because they are present on the same dishes, and the target cells are difficult to isolate. There was also the question of whether the presence of beating cells means differentiation to cardiomyocytes, or merely fusion with fetal cardiomyocytes. Since marrow cells spontaneously fuse with co-cultured ES cells *in vitro* [44], controversy has arisen as to whether regenerated myocardium represents transplanted cells fused with native cardiomyocytes instead of differentiated donor cells. Cell fusion did not occur in our study, however, because cardiomyogenic differentiation was demonstrated by the double-labeling of two types of co-cultured cells *in vitro*.

The co-culture of the target cells, i.e., the marrow stroma, in this study, on appropriate feeder cells may provide a good system for generating a source of cells for therapy. hMSCs have the ability to form tight cell-to-cell couplings, i.e., gap junctions, with adjacent hMSCs, suggesting that the grafted hMSCs are capable of generating electrical coupling and may function coordinately in the recipient human heart. On the other hand, the disorganization of the spontaneous beating rhythm in the early stage may result in arrhythmogenesis when grafted into the recipient. Early afterdepolarization, which triggers arrhythmias, has been reported in cardiomyocytes generated by ES cells or embryonal carcinoma cells [45]. By contrast, the absence of early afterdepolarization in hMSCs may be beneficial in terms of not leading to arrhythmias when the cells are transplanted *in vivo*. The rhythm of the hMSCs that underwent premature differentiation became regular after complete differentiation in the present study, and culture for a certain period therefore seems necessary before cell transplantation. It is noteworthy that the risk of lethal arrhythmia can be reduced by promoting electrical maturation of hMSCs *in vitro* when this co-culture system is used for therapy clinically.

It remains unresolved how co-cultured hMSCs start beating spontaneously and what the key factor(s) in cardiac differentiation are. Several factors promote differentiation into cardiomyocytes, such as gap junctions, humoral factors, electrical and mechanical stimulation, and cell-to-cell contact. Gap junctions have been shown to be necessary for differentiation of endothelial progenitor cells to cardiomyocytes [20], but the lack of gap junctional communication between hMSCs and feeder cells in our study indicates that gap junctions are not prerequisite for differentiation. In addition, separation of hMSCs and fetal cardiomyocytes in a co-culture system with a membrane that is permeable to humoral factors but not to cells resulted in loss of capacity for cardiac differentiation (data not shown), implying that humoral factors alone do not induce cardiac differentiation of hMSCs, and direct interactions, such as with cell-membrane bound molecules and extracellular matrix, seem to be essential. Cadherins, for example, have been reported to mediate calcium-dependent cell-to-cell contact and affect the differentiation of cardiac muscle cells [46]. Moreover, the decrease in number of beating hMSCs after the feeder cells stopped beating implies that mechanical stimulation in addition to cell-to-cell contact might be indispensable to cardiac differentiation and maintenance of the differentiated state.

Many clinical trials of regeneration therapy using mononuclear cells for the failing heart have been performed [13–16], but many more basic studies are needed. hMSCs with an expanded life span cannot be transplanted clinically, because they have been transduced with human papillomavirus E6 and E7 genes. The present results and others have shown that these molecules do not elicit cell transformation *in vitro*, at least during the period observed. This contrasts with human stromal cells being transformed during immortalization by SV40 large T antigen [47]. Based on the results of this study and the mechanism of cell life span extension, we are now developing a novel strategy to eliminate the possibility of transformation. Thus, cells that undergo reproducible cardiomyogenic differentiation and have a prolonged life span can be used as a good model of cell transplantation.

Acknowledgements

We would like to express our sincere thanks to K. Tsuchiya, T. Uyama and S. Matsumoto for support throughout the work, and T. Inomata, Y. Nakamura, and Y. Taki for providing expert

technical assistance. We are grateful to Dr. D. A. Galloway (FHCRC, Seattle, USA) for pLXSN-16E7 and to Dr. Y. Takeuchi (Chester Beatty Laboratories, ICR, UK) for the FLYA13 cells. This work was supported in part by a special grant for Advanced Research on Cancer from the Ministry of Education, Culture, Sports, Science, and Technology of Japan to T. K. and A. U., and the Organization for Pharmaceutical Safety and Research to A.U.

The cell names are summarized at http://1985.jukuin.keio.ac.jp/umezawa/cells/name.html. MPEG video stream of UBET-7 is available at http://1985.jukuin.keio.ac.jp/umezawa/jgm/ubet7.

References

1. Klug MG, Soonpaa MH, Koh GY, Field LJ. Genetically selected cardiomyocytes from differentiating embryonic stem cells form stable intracardiac grafts. *J Clin Invest* 1996; **98**: 216–224.
2. Min JY, Yang Y, Converso KL, *et al.* Transplantation of embryonic stem cells improves cardiac function in postinfarcted rats. *J Appl Physiol* 2002; **92**: 288–296.
3. Etzion S, Battler A, Barbash IM, *et al.* Influence of embryonic cardiomyocyte transplantation on the progression of heart failure in a rat model of extensive myocardial infarction. *J Mol Cell Cardiol* 2001; **33**: 1321–1330.
4. Muller-Ehmsen J, Whittaker P, Kloner RA, *et al.* Survival and development of neonatal rat cardiomyocytes transplanted into adult myocardium. *J Mol Cell Cardiol* 2002; **34**: 107–116.
5. Muller-Ehmsen J, Peterson KL, Kedes L, *et al.* Rebuilding a damaged heart: long-term survival of transplanted neonatal rat cardiomyocytes after myocardial infarction and effect on cardiac function. *Circulation* 2002; **105**: 1720–1726.
6. Ghostine S, Carrion C, Souza LC, *et al.* Long-term efficacy of myoblast transplantation on regional structure and function after myocardial infarction. *Circulation* 2002; **106**: I131–136.
7. Taylor DA, Atkins BZ, Hungspreugs P, *et al.* Regenerating functional myocardium: improved performance after skeletal myoblast transplantation. *Nat Med* 1998; **4**: 929–933.
8. Jackson KA, Majka SM, Wang H, *et al.* Regeneration of ischemic cardiac muscle and vascular endothelium by adult stem cells. *J Clin Invest* 2001; **107**: 1395–1402.
9. Orlic D, Kajstura J, Chimenti S, *et al.* Bone marrow cells regenerate infarcted myocardium. *Nature* 2001; **410**: 701–705.
10. Wang JS, Shum-Tim D, Galipeau J, Chedrawy E, Eliopoulos N, Chiu RC. Marrow stromal cells for cellular cardiomyoplasty: feasibility and potential clinical advantages. *J Thorac Cardiovasc Surg* 2000; **120**: 999–1005.
11. Shake JG, Gruber PJ, Baumgartner WA, *et al.* Mesenchymal stem cell implantation in a swine myocardial infarct model: engraftment and functional effects. *Ann Thorac Surg* 2002; **73**: 1919–1925; discussion 1926.
12. Gojo S, Gojo N, Takeda Y, *et al.* In vivo cardiovasculogenesis by direct injection of isolated adult mesenchymal stem cells. *Exp Cell Res* 2003; **288**: 51–59.
13. Strauer BE, Brehm M, Zeus T, *et al.* Repair of infarcted myocardium by autologous intracoronary mononuclear bone marrow cell transplantation in humans. *Circulation* 2002; **106**: 1913–1918.
14. Hamano K, Nishida M, Hirata K, *et al.* Local implantation of autologous bone marrow cells for therapeutic angiogenesis in patients with ischemic heart disease: clinical trial and preliminary results. *Jpn Circ J* 2001; **65**: 845–847.
15. Assmus B, Schachinger V, Teupe C, *et al.* Transplantation of progenitor cells and regeneration enhancement in acute myocardial infarction (TOPCARE-AMI). *Circulation* 2002; **106**: 3009–3017.
16. Tse HF, Kwong YL, Chan JK, Lo G, Ho CL, Lau CP. Angiogenesis in ischaemic myocardium by intramyocardial autologous bone marrow mononuclear cell implantation. *Lancet* 2003; **361**: 47–49.
17. Menasche P, Hagege AA, Scorsin M, *et al.* Myoblast transplantation for heart failure. *Lancet* 2001; **357**: 279–280.
18. Prockop DJ. Marrow stromal cells as stem cells for nonhematopoietic tissues. *Science* 1997; **276**: 71–74.
19. Makino S, Fukuda K, Miyoshi S, *et al.* Cardiomyocytes can be generated from marrow stromal cells in vitro. *J Clin Invest* 1999; **103**: 697–705.
20. Badorff C, Brandes RP, Popp R, *et al.* Transdifferentiation of blood-derived human adult endothelial progenitor cells into functionally active cardiomyocytes. *Circulation* 2003; **107**: 1024–1032.
21. Hayflick L, Moorhead PS. The serial cultivation of human diploid cell strains. *Exp Cell Res* 1961; **25**: 585–621.
22. Bruder SP, Jaiswal N, Haynesworth SE. Growth kinetics, self-renewal, and the osteogenic potential of purified human mesenchymal stem cells during extensive subcultivation and following cryopreservation. *J Cell Biochem* 1997; **64**: 278–294.
23. Kiyono T, Foster SA, Koop JI, McDougall JK, Galloway DA, Klingelhutz AJ. Both Rb/p16INK4a inactivation and telomerase activity are required to immortalize human epithelial cells. *Nature* 1998; **396**: 84–88.
24. Jacobs JJ, Kieboom K, Marino S, DePinho RA, van Lohuizen M. The oncogene and Polycomb-group gene bmi-1 regulates cell proliferation and senescence through the ink4a locus. *Nature* 1999; **397**: 164–168.
25. Lessard J, Sauvageau G. Bmi-1 determines the proliferative capacity of normal and leukaemic stem cells. *Nature* 2003; **423**: 255–260.
26. Park IK, Qian D, Kiel M, *et al.* Bmi-1 is required for maintenance of adult self-renewing haematopoietic stem cells. *Nature* 2003; **423**: 302–305.
27. Okamoto T, Aoyama T, Nakayama T, *et al.* Clonal heterogeneity in differentiation potential of immortalized human mesenchymal stem cells. *Biochem Biophys Res Commun* 2002; **295**: 354–361.
28. Kiyono T, Hiraiwa A, Fujita M, Hayashi Y, Akiyama T, Ishibashi M. Binding of high-risk human papillomavirus E6 oncoproteins to the human homologue of the Drosophila discs large tumor suppressor protein. *Proc Natl Acad Sci U S A* 1997; **94**: 11612–11616.
29. Imabayashi H, Mori T, Gojo S, *et al.* Redifferentiation of dedifferentiated chondrocytes and chondrogenesis of human bone marrow stromal cells via chondrosphere formation with expression profiling by large-scale cDNA analysis. *Exp Cell Res* 2003; **288**: 35–50.
30. Naviaux RK, Costanzi E, Haas M, Verma IM. The pCL vector system: rapid production of helper-free, high-titer, recombinant retroviruses. *J Virol* 1996; **70**: 5701–5705.
31. Halbert CL, DG Galloway DA. The E7 gene of human papillomavirus type 16 is sufficient for immortalization of human epithelial cells. *J Virol* 1991; **65**: 473–478.
32. Cosset F-LTY, Battini J-L, Weiss RA, Collins MKL. High-titer packaging cells producing recombinant retroviruses resistant to human serum. *J Virol* 1995; **69**: 7430–7436.
33. Yamashita T, Tonoki H, Nakata D, Yamano S, Segawa K, Moriuchi T. Adenovirus type 5 E1A immortalizes primary rat cells expressing wild-type p53. *Microbiol Immunol* 1999; **43**: 1037–1044.
34. Tomita S, Nakatani T, Fukuhara S, Morisaki T, Yutani C, Kitamura S. Bone marrow stromal cells contract synchronously with cardiomyocytes in a co-culture system. *Jpn J Thorac Cardiovasc Surg* 2002; **50**: 321–324.
35. Kohyama J, Abe H, Shimazaki T, *et al.* Brain from bone: efficient "meta-differentiation" of marrow stroma-derived mature osteoblasts to neurons with Noggin or a demethylating agent. *Differentiation* 2001; **68**: 235–244.
36. Pittenger MF, Mackay AM, Beck SC, *et al.* Multilineage potential of adult human mesenchymal stem cells. *Science* 1999; **284**: 143–147.
37. Jiang Y, Jahagirdar BN, Reinhardt RL, *et al.* Pluripotency of mesenchymal stem cells derived from adult marrow. *Nature* 2002; **418**: 41–49.
38. Romanov SR, Kozakiewicz BK, Holst CR, Stampfer MR, Haupt LM, Tlsty TD. Normal human mammary epithelial cells spontaneously escape senescence and acquire genomic changes. *Nature* 2001; **409**: 633–637.
39. Rheinwald JG, Hahn WC, Ramsey MR, *et al.* A two-stage, p16(INK4A)- and p53-dependent keratinocyte senescence mechanism that limits replicative potential independent of telomere status. *Mol Cell Biol* 2002; **22**: 5157–5172.

40. Bodnar AG, Ouellette M, Frolkis M, *et al.* Extension of life-span by introduction of telomerase into normal human cells. *Science* 1998; **279**: 349–352.
41. Taylor S, Jones PA. Multiple new phenotypes induced in 10T1/2 cells and 3T3 cells treated with 5-azacytidine. *Cell* 1979; **17**: 771–779.
42. Santi DV, Norment A, Garrett CE. Covalent bond formation between a DNA-cytosine methyl transferase and DNA containing 5-azacytidine. *Proc Natl Acad Sci U S A* 1984; **81**: 6993–6997.
43. Tomita S, Li RK, Weisel RD, *et al.* Autologous transplantation of bone marrow cells improves damaged heart function. *Circulation* 1999; **100**: II247–256.
44. Terada N, Hamazaki T, Oka M, *et al.* Bone marrow cells adopt the phenotype of other cells by spontaneous cell fusion. *Nature* 2002; **416**: 542–545.
45. Zhang YM, Hartzell C, Narlow M, Dudley SC Jr. Stem cell-derived cardiomyocytes demonstrate arrhythmic potential. *Circulation* 2002; **106**: 1294–1299.
46. Linask KK, Knudsen KA, Gui YH. N-Cadherin-catenin interaction: necessary component of cardiac cell compartmentalization during early vertebrate heart development. *Dev Biol* 1997; **185**: 148–164.
47. Harigaya K, Handa H. Generation of functional clonal cell lines from human bone marrow stroma. *Proc Natl Acad Sci U S A* 1985; **82**: 3477–3480.

Photon-Modulated Changes of Cell Attachments on Poly(spiropyran-*co*-methyl methacrylate) Membranes

Akon Higuchi,*,† Ayu Hamamura,† Yosuke Shindo,† Hanako Kitamura,† Boo Ok Yoon,† Taisuke Mori,‡ Taro Uyama,‡ and Akihiro Umezawa‡

Department of Applied Chemistry, Seikei University, 3-3-1 Kichijoji Kitamachi, Musashino, Tokyo 180-8633, Japan

Received May 1, 2004; Revised Manuscript Received June 2, 2004

Spiropyran is a photoresponsive molecule, and nonionic spiropyran is reversibly changed by UV irradiation to a hydrophilic polar, zwitterionic merocyanine isomer, and back again by visible light irradiation. A copolymer of nitrobenzospiropyran and methyl methacrylate, poly(NSP-*co*-MMA) was used as a material with a photosensitive surface. UV irradiation of the photosensitive surface of poly(NSP-*co*-MMA)-coated glass plates decreased the water contact angles (11 ± 1°) and increased diameter of a water drop relative to the unexposed surface. Light-induced detachment of platelets and mesenchymal stem (KUSA-A1) cells on poly(NSP-*co*-MMA)-coated glass plates was observed upon simple- and patterned-light irradiation, whereas no light-induced detachment of platelets and mesenchymal stem cells was observed on poly(methyl methacrylate)-coated glass plates. This is a result of the change from a closed nonpolar spiropyran to the polar zwitterionic merocyanine isomer induced by UV irradiation. Light-induced detachment of fibrinogen adsorbed on poly(NSP-*co*-MMA) coated glass plates was also observed in this investigation.

Introduction

In an effort to induce or control surface wetting by liquids, a number of researchers have proposed the use of a variety of means of changing the interfacial properties of materials including electrical potentials and fields,[1,2] temperature,[3,4] light,[5−7] and chemical means.[8] The focus of these studies has been on the manipulation of microchannels, micro-total analysis systems (μ-TAS),[9,10] and the capillary surface using external stimuli. Rosario et al. investigated the microfluidic actuation of water in capillary tubes coated with a photosensitive layer. Water in the capillary tubes was observed to rise on the order of 2.8 mm for a 500 μm diameter capillary, when the wavelength of incident light was switched from the visible region to the UV region. This is thought to be because the relatively nonpolar spiropyran can be reversibly switched to a polar, zwitterionic merocyanine isomer with a much larger dipole moment upon UV light irradiation, and back to the nonpolar spiropyran isomer again upon visible light irradiation.[7]

Surface control of hydrophilic/hydrophobic properties by external stimuli such as temperature change was also reported to develop thermo-responsive culture dishes for cells.[11,12] Hirose and Okano et al. developed designed shape cell sheets for tissue engineering in which human aortic endothelial cells were cultured and proliferated on tissue culture polystyrene dishes grafted with poly(*N*-isopropylacrylamide) (PIPAAm) and poly(*N*,*N*′-dimethylacrylamide) for thermosensitive response of cell adhesive and cell nonadhesive domains.[11] When the culture temperature was reduced below 32 °C (LCST), PIPAAm changed to hydrophilic and the cell sheets detached from PIPAAm-grafted surfaces in the absence of an enzyme such as trypsin.[11]

In this study, we investigated light-induced detachment of platelets and mesenchymal stem (KUSA-A1) cells on poly(NSP-*co*-MMA)-coated glass plates upon simple- and patterned-light irradiation as well as the change of physical properties on the photosensitive surface of poly(NSP-*co*-MMA)-coated glass plates, i.e., hydrophobicity−hydrophilicity change and change of amount of protein adsorption induced by UV irradiation.

Experimental Section

Preparation of Membranes. Poly(NSP-*co*-MMA) was synthesized by a conventional route according to the literature[17,18] and was donated by M. Kameda, K. Sumaru, and T. Kanamori (AIST).[19] Poly(NSP-*co*-MMA), 0.1 wt % in dichloroethane, was cast onto glass plates in flat Petri dishes. PMMA-coated glass plates were also prepared for use as controls.

Physical Characteristic Measurements. The water contact angles of the poly(NSP-*co*-MMA)-coated and PMMA-coated glass plates were measured at 25 °C and 85% relative humidity by the sessile drop method using ultrapure water.[20] The water contact angles were monitored and recorded with a CCD camera (DCR−PC100, Sony Corporation). At least four readings ($n = 4$) were taken at 2 min after placing water droplets (6−7 mm diameter) on different parts of the glass plates, and the values were averaged.

Fibrinogen Adsorption Assay. Fibrinogen adsorption from human plasma on the surface of the poly(NSP-*co*-

* To whom correspondence should be addressed. Tel: +81-422-37-3748. Fax: +81-422-37-3748. E-mail: higuchi@ch.seikei.ac.jp.
† Seikei University.
‡ National Center for Child Health and Development.

10.1021/bm049737x CCC: $27.50
Published on Web 07/07/2004

MMA)-coated and PMMA-coated glass plates was directly evaluated using the method based on the antigen−antibody reaction using enzyme-immunoglobulin conjugate (ELISA assay).[13] Briefly, the poly(NSP-*co*-MMA)-coated and PMMA-coated glass plates were immersed in 50% platelet-poor plasma diluted with phosphate buffer solution (PBS, 0.02M, pH 7.4) containing 0.15 mol/L NaCl for 180 min at 37 °C. After the poly(NSP-*co*-MMA)-coated and PMMA-coated glass plates were rinsed with sufficient PBS and were shifted into another new 24-well tissue culture flask, the poly(NSP-*co*-MMA)-coated and PMMA-coated glass plates were incubated with the primary antibody (i.e., mouse monoclonal anti-human fibrinogen (F4639, Sigma-Aldrich, Inc.)) diluted with Block Ace (UK−B80, Funakoshi Co.) solution for 1 h at 37 °C. Thereafter, the primary antibody was blocked with Block Ace solution after rinsing the glass plates with PBS containing 0.05 wt % Tween 20. The poly(NSP-*co*-MMA)-coated and PMMA-coated glass plates were subsequently incubated with the secondary antibody, rabbit H+L anti-mouse immunoglobulin peroxidase conjugate antibody (014−17611, Wako Pure Chemical Industries, Ltd.) for 60 min at 37 °C.

After sufficiently rinsing the poly(NSP-*co*-MMA)-coated and PMMA-coated glass plates with PBS containing 0.05 wt % Tween 20, 0.6 mL of a H_2O_2 solution containing the substrate for horseradish peroxidase, 3,3′,5,5′-tetramethylbenzidine (TMB Microwell Peroxidase Substrate System, 50−76−00, Kirkegaard & Perry Laboratories), was added to the 24-well tissue culture flask containing the glass plates. The absorbance of the solution was measured at 450 nm after 15 min of the enzyme reaction when the stop solution (1 mole/l H_3PO_4 solution) of the reaction was injected into the 24-well tissue culture flask. These measurements were carried out four times for each glass plates.

Light-Induced Detachment of Platelets. The poly(NSP-*co*-MMA)-coated glass plates in a 24-well tissue culture flask were equilibrated in saline solution at 37 °C for 1 h. The saline solution was removed, and 1 mL of fresh platelet-rich plasma (PRP)[13] was subsequently introduced into each well. The poly(NSP-*co*-MMA)-coated glass plates were incubated with PRP at 37 °C for 30 min. Then, the poly-(NSP-*co*-MMA)-coated glass plates were illuminated with UV irradiation using a handy UV lamp (UVGL-25, 365 nm, 950 μW/cm^2, UVP, Inc.) from the bottom of the 24-well tissue culture flask for 4 min at 37 °C. Control experiments in which the poly(NSP-*co*-MMA)-coated glass plates were not illuminated by UV irradiation were also performed. After 4 min, PRP was removed using a Pasteur pipet and 1 mL of PBS was pipetted into each well of the flask. The platelet numbers on both the poly(NSP-*co*-MMA)-coated glass plates, exposed to UV irradiation and not exposed to UV irradiation, were counted before and after UV irradiation using inverted phase-contrast microscopy (IX70, Olympus Corporation) equipped with a CCD video camera (CS230, Olympus Corporation). Light-induced detachment of platelets on PMMA-coated glass plates was also performed using the same procedures as a control. These measurements were carried out four times for each membrane.

Light-Induced Detachment of KUSA-A1 Cells. Mesenchymal stem cell line, KUSA-A1, derived from the bone marrow of female C3H/He mice (A. U.)[21] was used in this study. The poly(NSP-*co*-MMA)-coated glass plates in the 24-well tissue culture flask were equilibrated with saline solution at 37 °C for 1 h. The saline solution was removed, and 1 mL of KUSA-A1 cell suspension supplemented with DMEM media and 10% fetal bovine serum was subsequently introduced into each well. The poly(NSP-*co*-MMA)-coated glass plates were incubated with KUSA-A1 cells in a constant 5% CO_2 atmosphere at 37 °C for 30 min. Then, the poly(NSP-*co*-MMA)-coated glass plates were illuminated by UV light using the handy UV lamp (UVGL-25, 365 nm, 950 μW/cm^2, UVP, Inc.) from the bottom of the 24-well tissue culture flask for 4 min. When the patterned light irradiation was performed, a striped pattern mask (width; 2.5 mm), made from a transparency sheet (CG3410, 3M), was placed under the well. Additionally, control experiments in which the poly(NSP-*co*-MMA)-coated glass plates were not illuminated by UV irradiation were also performed. After 4 min, the DMEM media was removed using a Pasteur pipet and 1 mL of DMEM media was inserted into each well of the flask. The cell numbers of KUSA-A1 cells on both the poly(NSP-*co*-MMA)-coated glass plates, illuminated and not illuminated by UV irradiation, were counted before and after UV irradiation using inverted phase-contrast microscopy with CCD video camera. Light-induced detachment of KUSA-A1 cells on the PMMA-coated glass plates was also performed as a control according to the same procedure. These measurements were carried out four times for each membrane.

Results and Discussion

Hydrophobicity−Hydrophilicity Change. Hydrophilicity−hydrophobicity change induced by UV irradiation was investigated on poly(NSP-*co*-MMA) (see Figure 1) and poly-(methyl methacrylate) (PMMA) coated glass plates. Figure 2 shows the time dependence of the water contact angle and the diameter ratio (d_t/d_0) of the water drop on poly(NSP-*co*-MMA)-coated and PMMA-coated glass plates where d_0 and d_t are the diameter of water drop at time = 0 and t min after UV (375 nm) irradiation, respectively.

UV irradiation of the control surface of PMMA-coated glass plates demonstrated no change in the water contact angles within the experimental error and only a slight decrease in the diameter of the water droplet. The slight decrease of d_t/d_0 on the PMMA-coated glass plates was attributed to evaporation of water drop during the measurements. The photosensitive surface of poly(NSP-*co*-MMA)-coated glass plates under UV irradiation resulted in decreased water contact angles as well as an increased diameter of water droplet relative to that on the surface before UV light irradiation. The large change in the dipole moment between the two isomeric states of the spiropyran was determined to induce changes in the energy at the surface of poly(NSP-*co*-MMA). Spiropyran-coated photosensitive surfaces were determined to change in the surface energy solely upon light irradiation, as measured by the water contact angle.